Sahu Aresh (Orcid ID: 0000-0001-8673-9807)
Goldman Dan (Orcid ID: 0000-0002-0013-1188)

Notch signaling via Hey1 and Id2b regulates Müller glia's regenerative response to retinal injury

Running title: Notch signaling and retina regeneration

Aresh Sahu, Sulochana Devi, Jonathan Jui and Daniel Goldman*

Michigan Neuroscience Institute and Department of Biological Chemistry

University of Michigan, Ann Arbor, MI 48109

*Correspondence: Daniel Goldman, neuroman@umich.edu

Acknowledgments

This work was supported by grants from the NIH (NEI RO1 EY027310 and NEI RO1 EY032867) and the Gilbert Family Foundation Vision Restoration Initiative. We thank David Hyde, Notre Dame, for *gfap:GFP* transgenic fish; Michael Parsons, University California, Irvine, for *tp1:mCherry* transgenic fish; Mi-Sun Lee for generating *ubi:Cas9* transgenic fish; Elizabeth Mills for generating *u6:dll4-gRNAs*$_{1,2}$ and *u6:n3-gRNAs*$_{1,2}$ transgenic fish; Muchu Zhou and Zachary Rekowski for maintaining our zebrafish colony; and all members of the Goldman lab for their comments on this work. We also acknowledge and thank the University of Michigan's Cell Sorting Core, Advanced Genomics Core, and Bioinformatics Core. The authors declare no conflicts of interest.

Word count: Total word count (11,111); Abstract (150); Introduction (688); Materials and Methods (1938); Results (5007); Discussion (1374); References (2032); Figure Legends (1370); Supplemental Figure Legends (786).

Abstract

Zebrafish Müller glia (MG) respond to retinal injury by suppressing Notch signaling and producing progenitors for retinal repair. A certain threshold of injury-derived signal must be exceeded in order to engage MG in a regenerative response (MG's injury-response threshold). Pan-retinal Notch inhibition expands the zone of injury-responsive MG at the site of focal injury, suggesting that Notch signaling regulates MG's injury-response threshold. We found that Notch signaling enhanced chromatin accessibility and gene expression at a subset of regeneration-associated genes in the uninjured retina. Two Notch effector genes, *hey1* and *id2b*, were identified that reflect bifurcation of the Notch signaling pathway, and differentially regulate MG's injury-response threshold and proliferation of MG-derived progenitors. Furthermore, Notch signaling component gene repression in the injured retina suggests a role for Dll4, Dlb, and Notch3 in regulating Notch signaling in MG and epistasis experiments confirm that the Dll4/Dlb-Notch3-Hey1/Id2b signaling pathway regulates MG's injury-response threshold and proliferation.

Key words: stem cell, Ascl1, dll4, notch3, reprogramming, zebrafish

Main points:

- Notch represses chromatin accessibility & the expression of regeneration-associated genes in the uninjured retina.
- Hey1 regulates Müller glia's injury-response threshold; Hey1 & id2b regulate proliferation of Müller glia-derived progenitors.

Introduction

Although the mammalian and zebrafish retina share structure and function, only zebrafish are able to regenerate a damaged retina. Key to this regenerative response are Müller glia (MG) that normally contribute to retinal structure and homeostasis (Goldman, 2014; Lahne, Nagashima, Hyde, & Hitchcock, 2020; Lenkowski & Raymond, 2014; MacDonald et al., 2015; Reichenbach & Bringmann, 2013; Wan & Goldman, 2016). MG are the only retinal cells that exhibit a radial glial morphology with processes extending longitudinally and laterally that allow MG to interact with and sample their environment.

A needle poke injury to the zebrafish retina stimulates MG at the injury site to mount a regenerative response (Fausett & Goldman, 2006). This response includes changes in MG gene expression and signal transduction which precedes a self-renewing asymmetric cell division that produces a transient amplifying progenitor for retinal repair (Hoang et al., 2020; Lee, Wan, & Goldman, 2020; Nagashima, Barthel, & Raymond, 2013; Powell, Grant, Cornblath, & Goldman, 2013; R. Ramachandran, Fausett, & Goldman, 2010a; R. Ramachandran, Zhao, & Goldman, 2011, 2012; Sifuentes, Kim, Swaroop, & Raymond, 2016; Wan & Goldman, 2017; Wan, Ramachandran, & Goldman, 2012; Wan, Zhao, Vojtek, & Goldman, 2014; X. F. Zhao et al., 2014).

It remains unknown why mammalian MG cannot mount a regenerative response like their zebrafish counterparts. However, their basal state likely dictates their regenerative/stem cell potential. Recent studies comparing MG transcriptomes across species, as well as targeted perturbation of specific genes and signaling pathways, have identified differences between fish and mammalian MG gene expression programs (Elsaeidi et al., 2018; Hoang et al., 2020; Lee et al., 2020; Sifuentes et al., 2016). For example, Notch signaling is active in adult zebrafish MG (Elsaeidi et al., 2018; Lee et al., 2020; Wan & Goldman, 2017; Wan et al., 2012), but is dramatically reduced in adult mouse MG (Lee et al., 2020; Nelson et al., 2011; Riesenberg, Conley, Le, & Brown, 2018). Interestingly, Notch signaling helps maintain MG quiescence in zebrafish (Campbell et al., 2021; Conner, Ackerman, Lahne, Hobgood, & Hyde, 2014; Elsaeidi et al., 2018; Wan & Goldman, 2017; Wan et al., 2012).

Using the needle poke injury model we have shown that MG at the injury site engage in a regenerative response that is reflected in their cell division (Fausett & Goldman, 2006). This restricted MG response suggests injury signals do not travel far from the injury site and that a certain threshold of injury-derived signal must be exceeded to engage MG in a regenerative response (MG's injury-response threshold). Indeed, MG do not mount a regenerative response when cell death remains low (Iribarne, Hyde, &

Masai, 2019; Lessieur et al., 2019; Montgomery, Parsons, & Hyde, 2010). A clue to how this injury-response threshold is set comes from the observation that the zone of injury-responsive MG is expanded when a needle poke injury is combined with pan retinal Notch inhibition (Lee et al., 2020; Wan & Goldman, 2017; Wan et al., 2012). Thus, normally quiescent MG near an injury site are recruited to a regenerative response when Notch signaling is inhibited. These data indicate that Notch signaling not only controls the proliferation of MG and MG-derived progenitors (Campbell et al., 2021; Conner et al., 2014; Lee et al., 2020; Wan & Goldman, 2017; Wan et al., 2012), but also controls MG's injury-response threshold which represents one of the earliest consequences of MG reprogramming. Understanding the mechanism by which Notch signaling controls MG's injury-response threshold may provide clues for enhancing the regenerative potential of mammalian MG.

Here we report on studies investigating how Notch signaling regulates MG's injury-response threshold. We found that Notch signaling inhibition enhances chromatin accessibility and the expression of certain regeneration-associated genes in quiescent MG. Of these genes, two Notch target genes, *hey1* and *id2b*, were identified that mediate the effects of Notch signaling on retina regeneration. Interestingly, Hey1 regulates MG's injury-response threshold, while both Hey1 and Id2b regulate proliferation of MG-derived progenitors. Furthermore, we found that *hey1* and *id2b* are downstream targets of Dll4/Dlb-Notch3 signaling. Finally, our studies indicate that retention of sufficient Notch signaling that allows for transient suppression distinguishes pro-regenerative MG in zebrafish from non-regenerative MG in mice.

Materials and Methods

Experimental models

Zebrafish: Animal studies were approved by the University of Michigan's Institutional Animal Care and Use Committee. Zebrafish were kept at 26-28^{o}C with a 14/10 hr light/dark cycle. Adult male and female fish from 6 to 12 months of age were used in these studies. *1016 tuba1a:GFP*, *gfap:GFP*, *hsp70:DN-MAML-GFP, gfap:mCherry* and *tp1:mCherry*, fish were previously described(Fausett & Goldman, 2006; Johnson et al., 2016; Kassen et al., 2007; Parsons et al., 2009; L. Zhao et al., 2014). We generated *hsp70:dll4-P2A-GFP, hsp70:GFP-P2A-dlb, hsp70:GFP-P2A-hey1*, *hsp70:id2b-P2A-GFP, ubi:Cas9*, *u6:dll4-gRNAs$_{1,2}$* and *u6:n3-gRNAs$_{1,2}$* transgenic fish using standard recombinant DNA techniques and Tol2 vector backbone. Expression constructs were injected into single cell zebrafish embryos as previously

described (Fausett & Goldman, 2006). Fish were anesthetized in tricaine and retinas were injured with needle pokes (2-4 injuries/retina for analysis of proliferation and protein expression on retinal sections and 10 injuries/retina for PCR, ATACseq and RNAseq), as previously described(Fausett & Goldman, 2006).

Cell proliferation assays

To investigate cell proliferation, fish received an IP injection of EdU (10 μl of 10mg/ml stock) 3 hours before sacrifice and Click-It chemistry was used for detection as previously described (Wan & Goldman, 2017). Some fish received an IP injection of BrdU (20 mM) 3 hours before sacrifice which was detected using anti-BrdU immunofluorescence as previously described (Fausett & Goldman, 2006).

RNA isolation and PCR

Total RNA was isolated using Trizol (Invitrogen). cDNA synthesis and PCR reactions were performed as previously described (Fausett, Gumerson, & Goldman, 2008; R. Ramachandran et al., 2010a). Real-time qPCR reactions were carried out using Green 2x LO-ROX qPCR mix (ASI) on an iCycler real-time PCR detection system (BioRad). The ΔΔCt method was used to determine relative expression of mRNAs in control and injured retinas and normalized to either *gapdh* or *gapdh*$_s$ mRNA levels. Individual comparisons were done using unpaired 2-tailed Student t-test. ANOVA with Fisher's PLSD post hoc analysis was used for multiple parameter comparison. Error bars are standard deviation (SD).

ATACseq and RNAseq

ATACseq experiments were performed in triplicate, RNAseq experiments were done in triplicate except comparisons of uninjured and injured retina which were done in duplicate. We used uninjured *gfap:GFP* and *1016 tuba1a:GFP* transgenic fish at 2 days post injury (dpi) to investigate injury-dependent changes in MG. We used uninjured *gfap:GFP* fish treated with DMSO or DAPT for 24 hours, or *gfap:GFP* and *gfap:GFPgfap:GFP;hsp70:DN-MAML* fish treated with heat shock once every 6 hours over a 24 hour period to investigate Notch-dependent changes in MG. Fish were a mix of males and females. GFP+ MG dissociated from dissected fish retinas were FACS purified as previously described (Powell et al., 2013; R. Ramachandran et al., 2010a). Retinas were injured with 10 needle poke injuries and 12 injured *1016 tuba1a:GFP* retinas yielded ~70,000 GFP+ cells. Two retinas from uninjured *gfap:GFP* fish yielded ~225,000 GFP+ cells. For ATACseq nuclei were isolated from GFP+ cells; transposase treatment and PCR amplification were as previously described (Buenrostro, Wu, Chang, & Greenleaf, 2015). For RNAseq, RNA was purified from GFP+ cells and RNA quality and quantity analyzed on a Bioanalyzer (Agilent).

RNA rin numbers were above 8. polyA RNA was used prepare cDNA libraries that were generated by the U of M's Advance Genomics Core and DNA was sequenced on an Illumina NovaSeq 6000 platform. Sequencing reads were analyzed by the University of Michigan's Bioinformatics Core. Reads were mapped to the zebrafish genome (GRZc11). The number of reads for each expressed gene was determined and differentially expressed genes were restricted to those exhibiting at least a 1.5-fold difference in expression with threshold abundance greater than 5 Fragments Per Kilobase of transcript per Million mapped reads to eliminate very low abundant transcripts whose estimates of fold-change are unreliable. For each sample used in ATACseq experiments we obtained >25 million reads with alignment rates between 80-89%. Total peaks called were >125,000. Transcription site enrichment scores ranged from 7.2-9.9. Fraction of reads in peaks were >0.2. For RNAseq experiments each sample yielded >30 million reads with alignment rates of 80-85%. Differentially expressed genes had an adjusted P value ≤ 0.05, FDR ≤ 0.05, and a fold change $\geq \pm$ 1.5.

Bulk RNA-seq data analysis of MG and nonMG

MG RNAseq data generated from *gfap:GFP* transgenic fish treated +/- NMDA or intense light were obtained from Hoang et al., 2020. The original raw sequencing reads were processed by the authors as described (Hoang et al., 2020). Briefly, RNAseq libraries were prepared from FACS purified GFP+ MG and GFP- nonMG with a result of 45 to 55 million reads per library. Each condition contained two biological replicates, and FPKM were calculated using raw counts. Using this dataset, we identified genes of interest and the corresponding FPKM across samples were averaged and formulated into heat maps using R for visualization.

scRNAseq data analysis of control and NMDA-treated retinas

Retinal scRNAseq data from control and NMDA damaged fish retinas were obtained from Hoang et al., 2020. Briefly, the authors used Cell Ranger from 10x Genomics to map zebrafish reads from scRNAseq to the genome with an average of 1000 to 1500 genes and 2500 to 3250 unique molecular identifiers per cell. Variable genes were identified and clustered with K-nearest neighbors and shared nearest neighbor modularity optimization through Seurat. Doublets were eliminated with an in-house algorithm, and marker genes were used to annotate cell types for each cell cluster identified. Using this dataset, we identified the scaled and normalized average expression of our genes of interest across cell clusters, and the percentage of cells per cluster expressing these genes were calculated using R. Dot plots were created using Seurat for visualization.

CRISPR-based gene editing

Gene editing was performed as previously described (Hwang et al., 2013; Vejnar, Moreno-Mateos, Cifuentes, Bazzini, & Giraldez, 2016). Briefly, we used CRISPRscan to identify 3-6 gRNAs that target the gene of interest (Moreno-Mateos et al., 2015). gRNA DNA template synthesis using gRNA primer, universal primer, and *in vitro* transcription are as previously described (Vejnar et al., 2016). gRNAs are tested for editing efficiency by injecting single cell embryos with *in vitro* transcribed gRNA, along with Cas9-nanos RNA; 2-4 days later, editing efficiency is determined using genomic DNA in T7 endonuclease 1 (T7E1) mismatch detection assays and PCR (Sentmanat, Peters, Florian, Connelly, & Pruett-Miller, 2018). For stable gene editing in transgenic fish, we generated *Ubi:Cas9;cmlc2:GFP* (*Ubi:Cas9*) transgenic fish using standard recombinant DNA protocols and Tol2 vectors. We also generated Tol2 vectors harboring two gRNAs targeting a single gene under the control of two *u6a* promoters as previously described (Yin et al., 2015). We chose to express 2 gRNAs for each gene to improve editing efficiency and generate large deletions. Stable transgenic lines were established as previously described and are referred to as *u6:gene-gRNA*$_{1,2}$ (Fausett & Goldman, 2006). For gene editing in transgenic lines, *Ubi:Cas9* fish and *u6:gene-gRNA*$_{1,2}$ were bred to each other and *Ubi:Cas9;u6:gene-gRNA*$_{1,2}$ fish (F1 generation) were used for gene editing experiments. Gene editing in transgenic fish was confirmed by PCR and DNA sequencing. For gene editing in F0 fish, we injected zebrafish embryos with previously validated *in vitro* transcribed gRNAs$_{1,2}$ and *Cas9-nanos* mRNA. Embryos were raised to adults and genomic DNA from fin clips was used in T7E1 mismatch detection assay and PCR to confirm gene editing (Sentmanat et al., 2018). We obtained similar results regardless of whether genomic DNA was isolated from retina or fin clips.

MOs, gRNAs, and qPCR Primers used in this study

All MOs, gRNAs, and primers used in this study are listed in Table Supplement 7.

Morpholino (MO) functional assays

MOs were obtained from Gene Tools, LLC and the sequences are listed in Table Supplement 7. All MOs have a lissamine tag. Unless otherwise stated, MOs were used at 1 mM concentration. For testing splice blocking *dll4*-and *hey1*-targeting MO, we injected either control MO or experimental MO (~1ng) into single cell zebrafish embryos. RNA was extracted from embryos at 24-48hrs post injection and assayed for *dll4* or *hey1* mRNA by PCR. For testing *dlb*-, *n3*-, and *id2b*-targeting MOs, we generated *pCS2+dlb-EGFP*, *pCS2+n3-EGFP* and *pCS2+id2b-EGFP* constructs that contained either *dlb*, *n3*, or *id2b* MO target

site upstream of the EGFP initiator AUG. Plasmids were linearized with Not1 restriction enzyme and capped sense RNA was synthesized using SP6 RNA polymerase using Invitrogen's mMESSAGE mMACHINE^{TM} SP6 Transcription Kit (Invitrogen, #AM1340) according to manufactures directions. Following purification, the capped RNA was dissolved in nuclease free water containing 0.2% phenol red and injected with experimental or control MO into single cell zebrafish embryos. Each embryo received approximately 50 pg of RNA and 250 pg of control or experimental MO. MO's were delivered to adult fish via intravitreal injection at the time of retinal injury and cellular uptake was facilitated by electroporation as previously described (Fausett et al., 2008).

Luciferase assay

A 3kb region upstream of the *hey1* gene's transcription start site was amplified by PCR and cloned into Xho1/Kpn1 sites of the *pXP1* plasmid to create *3kb-hey1:luciferase*. Using Q5® Site-Directed Mutagenesis Kit (NEB, E0554), we generated mutations in each of the two most highly conserved Rbpj binding sites (m1 and m2, Fig. 7a). Mutations were confirmed by DNA sequencing. To study *hey1* promoter activity, we transfected HEK 293T cells plated in 24 well tissue culture plates with wt and mutant *3kb-hey1:luciferase*, +/- CMV:NICD and *SV40:Renilla* as internal control using lipofectamine 3000 (Invitrogen). Two days after transfection, cells were washed with PBS, lysed, and luciferase and Renilla activities measured using a Luminometer (Turner Biosystems). Luciferase activity was normalized to Renilla activity.

Heat shock and pharmacological inhibitors

For heat shock, fish were immersed in a water bath at 37^{o}C for 1 hr before returning to system water at 28^{o}C. For extended periods of heat shock, this was repeated every 6 hrs. To inhibit Notch signaling we used DAPT (Cayman, Cat # 13197) prepared in DMSO as a 10mM stock and diluted 1/250 in fish water for immersion. Control fish were treated with vehicle. Fish were exposed to DAPT for 24 hours.

Immunofluorescence and TUNEL assay

Zebrafish samples were prepared for immunofluorescence as previously described (Fausett & Goldman, 2006; R. Ramachandran et al., 2010a; R. Ramachandran, Reifler, A., Parent, J.M and Goldman, D., 2010). Primary antibodies used in this study: Rabbit anti-GFP, Thermo Fisher, Cat. # A6455 (1/1000); Mouse anti-mCherry, Abcam, Cat. # ab125096 (1:500); and mouse anti-glutamine synthetase (GS), Sigma-Aldrich, Cat. #MAB302 (1/500). Secondary antibodies used were: Alexa Flour 555 Donkey anti Mouse-IgG (H+L), Thermo Fisher Cat. # A31570 (1:500); Alexa flour 555 Donkey anti Rabbit IgG (H+L), Thermo

Fisher, Cat # A31572 (1:500); Alexa Flour 488 donkey anti mouse Thermo Fisher Cat. # A21202 (1:500); Alexa Flour 488 goat anti rabbit Thermo Fisher Cat. # A11008 (1:500).

We used an *in situ* Cell Death Fluorescein Kit (Millipore Sigma, Cat. # 11684795910) to detect apoptotic cells.

Microscopy and cell quantification

Images were captured by a Zeiss Axiophot fluorescence microscope or a Leica DM2500 microscope. EdU and BrdU labelling were used to identify and quantify proliferating cells in retinal sections as previously described (Fausett & Goldman, 2006; R. Ramachandran et al., 2010a; Wan & Goldman, 2017; Wan et al., 2012; Wan et al., 2014). The width of the proliferative zone was quantified at the center of the injury site where the largest number of proliferating cells reside.

Statistical analysis

Unless otherwise indicated, sample size is 3 fish and experiments were repeated at least 3 times. Statistical analyses were performed in GraphPad Prism. Error bars are standard deviation (SD). Two-tailed Student's *t* test was used for single parameter comparison; all measurements were taken from distinct samples.

Data sharing

Raw data have been deposited in GEO under the superset accession number GSE160179 and will be released upon acceptance of manuscript for publication.

Results

Notch signaling in developing and adult zebrafish

In the adult zebrafish retina, Notch signaling is restricted to quiescent MG where it regulates MG's regenerative response (Elsaeidi et al., 2018; Wan & Goldman, 2017). In the mammalian retina *Hes5* expression, which is used as a proxy for Notch signaling activity, is detected in MG at P7; however, by P30 this expression is reduced to very low levels with endogenous *Hes5* expression reaching the limits of detection (Nelson et al., 2011). Furthermore, although *Hes5:GFP* transgenic mice indicate a low level of Hes5 expression in mouse MG at P21-30 (Nelson et al., 2011; Riesenberg et al., 2018), these very low levels of Hes5 expression are not impacted by inhibitors of Notch signaling (Elsaeidi et al., 2018).

Importantly, the reduced Notch signaling activity associated with maturing MG in the mouse retina correlates with a loss in their regenerative potential (Loffler, Schafer, Volkner, Holdt, & Karl, 2015).

To compare this mammalian pattern of retinal Notch signaling during development with that of fish, we crossed *tp1:mCherry* Notch reporter fish with *gfap:GFP* fish that label MG (Kassen et al., 2007; Parsons et al., 2009). In developing fish, mCherry and GFP immunofluorescence indicate Notch signaling is activated and restricted to differentiating MG within the first 2 days post-fertilization (dpf), preceding *gfap:GFP* transgene induction (Figure 1A). mCherry immunofluorescence was not detect in progenitors residing in the retinal periphery. PCR analysis of retinal *mCherry* RNA levels indicates a gradual reduction in Notch signaling as the fish matures (Figure 1B and 1C). Nonetheless, unlike that of mouse MG, residual Notch signaling in adult zebrafish MG is readily detected and regulated by retinal injury, γ-secretase inhibitors, and dominant-negative MAML (DN-MAML) (Figures 1B-G)(Elsaeidi et al., 2018; Wan & Goldman, 2017). Thus, a major distinction between pro-regenerative MG in zebrafish and non-regenerative MG of mammals is the level of Notch signaling that is retained into adulthood.

Injury-dependent regulation of MG gene expression and chromatin accessibility

Although a relatively thorough characterization of MG gene expression and chromatin accessibility accompanying light- or NMDA-induced retinal degeneration was recently reported (Hoang et al., 2020), the impact of Notch signaling on these events was not investigated. Importantly, the mechanism by which Notch signaling regulates MG's responsiveness to injury-derived factors (MG's injury-response threshold) remains unexplored. We hypothesized that Notch signaling controls MG's injury-response threshold by impacting chromatin accessibility and gene expression at a subset of regeneration-associated genes. To identify these genes, we searched RNAseq data sets for genes responding to both injury and Notch manipulation, reasoning that this will provide candidate genes that regulate MG's injury-response threshold and proliferation.

To identify injury-responsive genes following needle poke injury, we compared RNAseq data sets from GFP+ MG that were FACS purified from the uninjured retina of *gfap:GFP* fish with those from *1016 tuba1a:GFP* fish at 2 days post injury (dpi) when most MG are in an activated state with some beginning to undergo cell division (Fausett & Goldman, 2006; Lee et al., 2020). Differential gene expression analysis identified 4,425 injury-responsive genes with 2,579 showing increased expression (fold change $\geq \pm 1.5$; Figure 2A). A small subset of these genes were validated by PCR (Figures 2B and S1A). Some of these genes, like *ascl1a* and *hbegfa,* were previously shown to regulate injury-dependent MG

proliferation and retina regeneration (Fausett et al., 2008; Gorsuch et al., 2017; R. Ramachandran et al., 2010a; R. Ramachandran et al., 2011; Wan et al., 2012).

ATACseq was used to assay chromatin accessibility changes as MG transition from a quiescent to an activated state following retinal injury. For this, GFP+ MG and GFP+ activated MG were FACS purified from uninjured *gfap:GFP* fish and injured *1016 tuba1a:GFP* fish (2 dpi), respectively, and nuclei were used for ATACseq (Buenrostro et al., 2015). We mapped injury-dependent differential chromatin accessibility to 5,684 genes (Figure 2C). On a global scale, ATACseq revealed a slight bias towards open chromatin in activated MG with 15,595 regions exhibiting an increase and 13,049 regions exhibiting a decrease in chromatin accessibility. Quantification of the number of unique annotations for each region and annotating these regions to different genic features revealed increased chromatin accessibility at intergenic regions and decreased chromatin accessibility at 5' UTR, promoters, and 1-5 kb region upstream of transcription start sites (Figure S1B).

To correlate injury-dependent changes in gene expression with chromatin accessibility, we intersected our RNAseq and ATACseq injury-regulated gene lists. This analysis identified 1,311 injury-responsive MG genes with changes in chromatin accessibility (Figures 2D and S1C). ~60% of the injury-induced genes and ~64% of the injury-repressed genes showed a corresponding change in chromatin accessibility (Figure 2D; Table S1). Importantly, many of these changes in chromatin accessibility included promoters and upstream sequences (Figure S1B and S1C; Table S2).

DAPT-dependent regulation of MG gene expression and chromatin accessibility

Notch repression with DAPT allows normally quiescent MG adjacent to the injury affected zone to mount a regenerative response(Wan & Goldman, 2017; Wan et al., 2012). To understand how Notch inhibition accomplishes this, we used RNAseq to characterize the DAPT-regulated transcriptome in quiescent MG. For this, GFP+ MG were FACS purified from uninjured *gfap:GFP* fish treated +/-DAPT for 24 hours. RNAseq identified 1,261 differentially expressed genes, of which 375 were reduced following Notch inhibition and 245 were also regulated by retinal injury (fold change $\geq \pm 1.5$; Figure 3A and 3B). Interestingly, these latter genes include *ascl1a* and *hbegfa* which are known to be essential for retina regeneration (Figures 3A, S2A, and S2B; Table S3) (R. Ramachandran et al., 2010a; R. Ramachandran et al., 2011; Wan et al., 2012).

We next used ATACseq to investigated the consequence of Notch signaling inhibition on MG chromatin accessibility (Buenrostro et al., 2015). For this, nuclei were isolated from GFP+ MG purified from

uninjured *gfap:GFP* fish treated +/-DAPT. On a global scale, inhibition of Notch signaling affected chromatin accessibility in a similar fashion as retinal injury with 16,990 regions showing increased and 12,413 regions showing decreased chromatin accessibility (Figure 3C). However, unlike that found with retinal injury, quantification of the number of unique annotations for each region and annotating these regions to different genic features revealed that DAPT-treatment increased chromatin accessibility in 5' regions of genes including 5'UTR, promoters, and 1-5kb upstream regions, while intergenic regions appear to be enriched for closed chromatin (Figure S2C and S2D).

We mapped DAPT-dependent differential chromatin accessibility to 7,643 genes (Figure 3D), which exceeds those whose chromatin accessibility is regulated by retinal injury (Figure 1D). Interestingly, when examining promoter regions (1kb upstream of transcription start site) for differential chromatin accessibility, we found 156 promoters with reduced chromatin accessibility, and 3,871 promoters with increased chromatin accessibility (Table S4). This bias towards open chromatin was also observed in the 1-5kb region upstream of transcription start sites, where we observed 196 genes with reduced chromatin accessibility and 1,041 genes with increased chromatin accessibility (Table S4).

Of the genes whose chromatin accessibility changed with DAPT-treatment, the expression of 1,497 were also regulated by retinal injury (Figure 3D), which is similar to the number of genes showing changes in chromatin accessibility after retinal injury (Figure 2D). However, when we correlate injury-dependent gene regulation with changes in chromatin accessibility upstream of transcription start sites, we found a larger proportion of the injury-responsive genomic regions with increased chromatin accessibility following DAPT-treatment compared to retinal injury (1,175 vs 642) (Figures 2D and 3D; Tables S2 and S4). Furthermore, ~67% of these latter increases in chromatin accessibility are associated with genes whose expression is increased in the injured retina.

Together, the above data suggests Notch inhibition in the uninjured retina contributes to lowering MG's injury-response threshold by increasing chromatin accessibility and regulating the expression of certain key regeneration-associated genes.

Notch-dependent regulation of genes impacting MG reprogramming

We hypothesized that MG regeneration-associated genes that are also regulated in a similar direction by Notch signaling in the uninjured retina would identify a relatively small set of genes that may regulate MG's injury-response threshold. Intersection of injury and Notch-regulated RNAseq data sets revealed 190 induced (basal value $\geq$5; fold change $\geq$1.5) and 55 repressed (basal value $\geq$50; fold change ≥1.5)

genes (Figures 3B, S2A, and S2B; Table S5). The top 20 injury-responsive genes that were regulated in similar direction following DAPT-treatment are listed in Figure S2A.

DAPT is a γ-secretase inhibitor that can target over 100 substrates, of which Notch is only one (Xia, 2019). To help narrow-in on Notch-regulated genes, we took advantage of *hsp70:DN-MAML* transgenic fish (L. Zhao et al., 2014). DN-MAML suppresses endogenous Notch-dependent gene activation (Maillard et al., 2006; Maillard et al., 2004). To identify MG genes regulated by DN-MAML in uninjured retina, we treated *gfap:mCherry* and *gfap:mCherry;hsp70:DN-MAML* fish with heat shock every 6 hours for 1 day and then FACS purified GFP+ MG for RNAseq. Expression analysis identified 1,122 differentially expressed genes with only 244 showing reduced expression (fold change $\geq \pm 1.5$; Figure S2E).

We next determined the intersection of injury-responsive MG genes that were also regulated in the same direction by DAPT and DN-MAML in the uninjured retina. Remarkably, this analysis identified 84 induced genes and 5 repressed genes (fold change $\geq \pm 1.5$) (Table S5 and genes marked with asterisk in Figure S2A). Thus, out of a total of 4,425 regeneration-associated genes, we have narrowed-in on 89 that are Notch-responsive in the uninjured retina and perhaps regulating MG's injury-response threshold.

Hey1 and Id2b regulate MG's injury-response threshold and proliferation

hey1 and *id2b* were the only transcriptional regulators consistently repressed with retinal injury or Notch inhibition, making them good candidates for being direct Notch target genes. Inspection of the 3kb region upstream of their transcriptional start sites revealed consensus Rbpj binding elements in the *hey1* gene (Figure 4A). Two of these elements are highly conserved in sequence and position when compared with orthologous genes from mouse and human (Figure 4A). Mutation of either of these putative Rbpj binding sites in a 3kb *hey1* promoter fragment driving luciferase gene expression resulted in a dramatic reduction in promoter activation by NICD when assayed in transfected HEK293 cells (Figure 4A and 4B).

To investigate if Hey1 and Id2b contributed to MG's injury-response threshold, we knocked down their expression with either a splice blocking *hey1*-morpholino (MO) or a translation blocking *id2b*-MO (Figure S3A-C). MO effectiveness was determined in embryos, where injection of the *hey1*-MO resulted in *hey1* RNA intron-retention and injection of the *id2b*-MO with an *id2b*-GFP chimeric RNA resulted in reduced GFP expression (Figure S3B and S3C). Remarkably, only Hey1 knockdown expanded the zone of injury-responsive MG (Figures 4C-E, and S3D). We confirmed this result using a CRISPR-based gene editing

strategy where embryos were injected with *in vitro* transcribed *Cas9-nanos* and 2 different gRNAs targeting either *hey1* or *id2b* exons 1 and 2 (Figure S3A). These fish were raised to adults and gene deletions were confirmed using genomic DNA from fin clips (Figure S3E and F). Consistent with our knockdown experiments, only editing of the *hey1* gene resulted in an expanded zone of injury-responsive MG (Figure 4F-H), which was not accompanied by changes in retinal cell death (Figure S3G).

Although only Hey1 regulated MG's injury-response threshold, both Hey1 and Id2b suppressed MG proliferation without affecting cell death in *hsp70:GFP-P2A-hey1* or *hsp70:id2b-P2A-GFP* fish (Figure 4I; Figure S3H). Hey1 overexpression also suppressed injury-dependent induction of regeneration-associated genes like *ascl1a* and *lin28a* (Figure 4J).

Together, the above data show that Notch-regulated genes affecting MG proliferation, like *id2b*, do not necessarily affect MG's injury-response threshold. However, genes that regulate MG's injury-response threshold, like *hey1*, also regulate the number of MG engaged in a proliferative response. These data suggest *hey1* and *id2b* reflect a bifurcation in Notch signaling.

Injury-dependent changes in Notch signaling component gene expression

We previously reported that *hey1* repression correlates with *dll4* repression in the injured retina (Wan & Goldman, 2017). Thus, based on the above data, Dll4 may regulate Notch signaling and MG's injury-response threshold. Indeed, of all Notch ligand encoding RNAs expressed in the retina, *dll4* is the most abundant and its injury-dependent suppression exceeds that of any other Notch ligand encoding gene (Figures 5A, 5B, and S4A)(Campbell et al., 2021; Hoang et al., 2020). Importantly, this suppression temporally follows Notch signaling repression (Figures 1F and 5B). However, contrary to the idea that Dll4 regulates MG's injury-response threshold is the observation that Dll4 knockdown inhibited proliferation of MG-derived progenitors in the light damaged retina, while Dlb knockdown enhanced this proliferation (Campbell et al., 2021). Campbell et al., also reported that *dlb* is enriched in the neuronal population, while *notch3* is enriched in the MG population, suggesting Dlb-Notch3 signaling controls MG quiescence (Campbell et al., 2021).

We were puzzled by the finding that *dlb*, whose overall basal expression and injury-dependent suppression is less than that of *dll4* would be the predominant regulator of Notch signaling in quiescent MG. One possibility is that *dlb* expression exceeds that of dll4 in a pan neuronal fashion, while dll4 expression is restricted to a subset of neurons and/or other cell types. Therefore, we queried previously generated bulk RNAseq data sets from MG and nonMG, and scRNAseq data sets from uninjured and

light or NMDA-damaged retina (Hoang et al., 2020). This analysis revealed that *dll4* expression exceeds that of *dlb* in both MG and nonMG populations and that *notch3* was enriched in the MG population (Figure 5C). Importantly, retinal injury suppressed *dll4* in both the MG and nonMG population, while *dlb* was less affected (Figure 5D). As controls, we evaluated *elavl3* and *ascl1a* expression - *elavl3* is an amacrine and ganglion cell marker, while *ascl1a* is a marker of activated and proliferating MG and MG-derived progenitors (Figure 5D).

Further interrogation of scRNAseq data sets indicated *dlb* and *dll4* are expressed at low levels in MG, resulting in only a small fraction of MG exhibiting expression above background (Figures 5E, S4B, and S4C). Nonetheless, in the uninjured retina, *dlb* is enriched in progenitors located in the ciliary margin and activated MG, while *dll4* predominates in the vascular endothelial (V/E) population (Figures 5E, S4B, and S4C). Both genes are poorly expressed in MG, neurons, and microglia; however, *dll4* expression exceeds that of *dlb* in these cells and is suppressed to various extents in each population following injury (Figure 5E, S4B and S4C). In contrast, *notch3* expression is highest in the pericyte and MG population and this MG expression is reduced after injury (Figure 5E). As expected, scRNAseq data sets show induction of *ascl1a* in activated MG following retinal injury, while *elavl3* expression is constitutively expressed in amacrine (AC) and retinal ganglion cell (RGC) populations (Figure S4C). The increased expression of *ascl1a* in resting MG after injury indicates that a fraction of these cells are in an activated state.

The above analysis raises the interesting possibility that neurodegeneration in the retina impacts V/E cells to control *dll4* expression. The relatively high basal expression of *dll4* in V/E cells and its coordinate repression with *notch3* and Notch signaling in MG suggests a mechanism for regulating Notch signaling in MG. Indeed, MG end-feet are in direct contact with V/E cells (Alvarez et al., 2007). Importantly, both photoreceptor degeneration in the light damaged retina and degeneration of amacrine and RGCs in the NMDA damaged retina reduce *dll4* expression in V/E cells (Figure 5E) (Hoang et al., 2020). However, cell type-specific *dll4* and *dlb* gene knockdown or inactivation in MG, V/E cells, neurons, and microglia is necessary to confidently identify the cell sources controlling Notch signaling in MG.

Notch signaling inhibits proliferation of MG-derived progenitors

The above studies presented a conundrum in that *dll4* gene expression suggested it might contribute to the maintenance of Notch signaling in quiescent MG, yet its knockdown was reported to inhibit proliferation of MG-derived progenitors (Campbell et al., 2021). Furthermore, it seemed odd that knockdown of *dll4* expression, which is already repressed to very low levels after retinal injury, would

have a similar effect on proliferation of MG-derived progenitors as repression of *dla*, *dlc*, or *dld* whose expression is highly induced in the injured retina (Figures 5A, 5B, and S4A) (Campbell et al., 2021). Finally, this latter result is at odds with a previous study showing conditional expression of NICD at 3-4 dpi inhibited proliferation of MG-derived progenitors (Wan et al., 2012), which is consistent with Notch signaling inhibiting proliferation or MG-derived progenitors. Thus, a further analysis of the role Dll4 and Notch signaling play in retina regeneration seemed warranted.

To further explore the relationship between Notch signaling and proliferation of MG-derived progenitors, we injured fish retinas with needle poke and labelled proliferating cells at 2 dpi with an intraperitoneal (IP) injection of EdU. Fish were then immersed in either DMSO or DAPT for an additional 2 days before receiving an IP injection of BrdU 3hrs prior to sacrifice. Quantification of the fraction of EdU+ cells that continued to proliferate at 4 dpi (BrdU+ & EdU+) revealed enhanced proliferation of MG-derived progenitors when Notch signaling was inhibited (Figure S4D). This result is most consistent with the idea that Notch signaling promotes quiescence of MG and MG-derived progenitors. Thus, we propose that the return of Notch signaling to the injured retina around 4 dpi (Figure 1F), which parallels the large increase in expression of *dla*, *dlc*, and *dld* (Figures 5B and S4A), facilitates progenitor cell cycle exit and differentiation.

Dlb, Dll4 and Notch3 regulate MG's injury-response threshold

Based on the above data, we hypothesized that Dll4 is a major regulator of Notch signaling in quiescent MG and thereby, regulates MG's injury-response threshold. To investigate this, we knocked down Dll4 using a *dll4*-MO that blocks *dll4* splicing and results in intron retention (*dll4*-MO, Figures 6A and S5H). Indeed, Dll4 knockdown increased MG proliferation and expanded the zone of proliferating MG in a concentration-dependent manner without affecting cell death (Figure 6B-E). In light of previous data indicating Dll4 knockdown stimulates proliferation of MG-derived progenitors (Campbell et al., 2021), it was important to verify this result with an independent method. For this we used a CRISPR-based strategy to edit the *dll4* gene. gRNAs were designed to target *dll4*'s DSL domain that interacts with the Notch receptor extracellular domain (gRNAs 1 and 2, Figure 6a). gRNAs were cloned into a Tol2 vector that allows expression of multiple gRNAs from different *u6* promoters (Yin et al., 2015), and these fish were named *u6:dll4-gRNA*$_{1,2}$. These fish were bred with *ubi:Cas9* transgenic fish to generate *ubi:Cas9;u6:dll4-gRNA*$_{1,2}$ fish. Fish harboring *dll4* gene deletions were identified by PCR using genomic DNA (Figure S5I). Like Dll4 knockdown, *dll4* gene editing resulted in an expanded zone of injury-responsive proliferating MG without affecting cell death (Figure 6F-6I). Finally, forced expression of Dll4

with heat shock in *hsp70:dll4-P2A-GFP* transgenic fish inhibited injury-dependent proliferation of MG and MG-derived progenitors, and also reduced the zone of proliferating MG without affecting retinal cell death (Figures 6J-6M and S5J). Together, these data suggest Dll4 regulates MG's injury-response threshold.

Although basal expression and injury-dependent repression of *dlb* is significantly less than *dll4* (Figure 5), Dlb knockdown results in increased MG proliferation in the injured retina, suggesting it too may contribute to MG's injury-response threshold (Campbell et al., 2021). To directly test this, we used a translation blocking MO to suppress Dlb in the needle poke injured retina. The *dlb*-MO was validated in zebrafish embryos injected with a *dlb-GFP* chimeric transcript (Figure S5A-S5D). Following Dlb knockdown, we noted an expanded zone of proliferating MG (Figure S5B-S5D). Furthermore, Dlb overexpression in *hsp70:GFP-p2A-dlb* fish, inhibited injury-dependent proliferation of MG-derived progenitors (Figure S5F and S5G).

Notch3 knockdown was previously reported to stimulate MG proliferation in the injured retina (Campbell et al., 2021), suggesting it may contribute to MG's injury-response threshold. Indeed, using a translation-blocking MO that suppressed chimeric *notch3-GFP* RNA expression, we observed an expanded zone of injury-responsive MG in the injured retina (Figure S6A-S6F). We confirmed this result using a CRISPR-based strategy to delete the *notch3* gene's ankyrin repeat domain that is required for recruiting MAML to the Rbpj-NICD complex ($gRNA_1$ and $gRNA_2$, Figure S6A and S6G) (Nam, Sliz, Song, Aster, & Blacklow, 2006). Retinal injury in *ubi:Cas9;u6:n3-gRNA$_{1,2}$* fish resulted in an expanded zone of injury-responsive MG and increased MG proliferation without affecting retinal cell death (Figure S6H-S6K).

Together, the above data are consistent with the idea that Dll4 and Dlb acting through Notch3 regulate Notch signaling in MG, which impacts MG's injury-response threshold.

Epistasis experiments suggest bifurcation of Notch signaling via regulated expression of *hey1* and *id2b*

The above studies suggested Dll4 and Dlb engage the Notch3 receptor to stimulate Hey1 and Id2b expression and that Hey1 regulates MG's injury-response threshold, while Id2b regulates the proliferation of MG-derived progenitors (Figure 4C-4I). To further investigate these gene interactions, we performed epistasis experiments and assayed the zone of injury-responsive MG and MG proliferation at 2 dpi when MG are beginning to proliferate (Fausett & Goldman, 2006). Consistent with Notch3 acting downstream of Dll4 and Dlb, we found that Notch3 knockdown expanded the zone of

proliferating MG in transgenic fish overexpressing Dll4 or Dlb. This was also reflected by an increase in proliferation of MG and MG-derived progenitors (Figure 7A and 7B). Interestingly, when we tested if Hey1 and Id2b acted downstream of these Notch signaling components, we found only Hey1 was able to suppress the expanded zone of injury-responsive MG resulting from knockdown of Dll4, Dlb, and Notch3, and this was also reflected in reduced proliferation of MG and MG-derived progenitors (Figure 7C and 7D). However, a small effect of Id2b overexpression on EdU+ cells in the control MO treated retina was noted (Figure 7C), which is consistent with Id2b suppressing progenitor proliferation at 4 dpi (Figure 4I).

Together out data suggest that a Dll4/Dlb-Notch-Hey1 signaling pathway regulates both MG's injury response threshold and proliferation, while a Dll4/Dlb-Notch-Id2b signaling pathway predominantly regulates proliferation of MG-derived progenitors. Thus, Hey1 and Id2b reflect a bifurcation of the Notch signaling pathway where downstream effectors have unique and overlapping consequence on retina regeneration.

Discussion

In the zebrafish retina, Notch signaling is restricted to quiescent MG. Following retinal injury, Notch signaling is suppressed in MG that engage in a regenerative response. Notch signaling regulates injury-dependent proliferation of MG and MG-derived progenitors (Campbell et al., 2021; Conner et al., 2014; Elsaeidi et al., 2018; Lee et al., 2020; Wan & Goldman, 2017; Wan et al., 2012), and our studies suggest Notch signaling also regulates MG's injury-response threshold (Wan & Goldman, 2017; Wan et al., 2012). This predicts a gradient of injury-derived factors that must exceed a certain level in order to engage MG in a regenerative response (Figure 8B). Indeed, low levels of neuron death do not stimulate MG proliferation (Iribarne et al., 2019; Lessieur et al., 2019; Montgomery et al., 2010). Our studies indicate that the amount of injury-related factors needed to elicit a regenerative response is determined in part by the basal level of Notch signaling in MG (Figure 8B).

In this report, we focused on mechanisms underlying these Notch-regulated processes. Our data suggests that Notch signaling reduces chromatin accessibility and expression of a subset of regeneration-associated genes to ensure that MG do not inappropriately enter a regenerative response (Figure 8A). By intersecting MG RNAseq gene lists from injured retina with those from uninjured retina +/- Notch inhibition, we identified Hey1 and Id2b as regeneration-associated, Notch-regulated genes.

Our data suggest that Hey1 and Id2b reflect a split in the Notch signaling pathway where Hey1 impacts MG's injury-response threshold and Id2b impacts proliferation of MG-derived progenitors. In an effort to identify genes that stimulate Notch signaling in the uninjured retina, we focused on the most highly expressed Notch ligand and receptor encoding genes in quiescent MG. This analysis revealed that in addition to Dlb (Campbell et al., 2021), Dll4 is a potent regulator of MG's injury response threshold and proliferation. We confirmed a Dll4/Dlb-Notch3-Hey1/Id2b signaling cascade using epistasis experiments and found that Notch inhibition from 2-4 dpi enhanced proliferation of MG-derived progenitors. Finally, our data suggest that the level of Notch signaling in MG appears to distinguish pro-regenerative MG of the zebrafish retina from non-regenerative MG of mammals.

We previously reported that Notch inhibition is insufficient to drive MG proliferation in the uninjured retina (Elsaeidi et al., 2018), and our analysis of Notch-regulated gene expression in quiescent MG suggests this may result from incomplete activation of the regeneration-associated transcriptome. Indeed, *lin28a*, a critical regeneration-associated gene is not induced following Notch inhibition in the uninjured retina. However, when Notch inhibition is combined with other factors, like Tnfa or Ascl1a and Lin28a, MG proliferation is observed (Conner et al., 2014; Elsaeidi et al., 2018). Thus, Notch signaling repression appears to license MG to engage in a proliferative response, and when exposed to sufficient levels of injury-related factors, MG enter a proliferative phase.

Although Dll4 and Dlb stimulate Notch signaling in quiescent MG, we suspect Dll4 may be the main endogenous factor regulating this process due to its relatively high basal expression, its robust repression following injury, and its better correlation with Notch signaling levels. Queried scRNAseq data sets indicate both genes are expressed at low levels in MG, activated MG, neurons, and microglia. However, *dll4* expression exceeds that of *dlb* in MG and neurons and both genes are barely detectable in microglia. Interestingly, *dlb* expression predominates in activated MG and progenitor populations, while *dll4* predominates in the V/E population. In addition, injury-dependent suppression of *dll4* was most robustly observed in the MG, neuronal, and V/E cell populations, while *dlb* repression was restricted to the activated MG population.

Injury-dependent regulation of *dll4* expression in V/E cells raises the interesting possibility that neuronal injury is communicated indirectly to MG via endothelial cells that make contact with MG end-feet. Indeed, rod loss has been associated with remodeling of the neurovascular unit, as are changes in neural activity (Attwell et al., 2010; Garhofer et al., 2020; Ivanova, Alam, Prusky, & Sagdullaev, 2019). However,

without cell type-specific gene inactivation we cannot distinguish if Notch signaling in MG is regulated by Notch ligands expressed in MG, neurons, V/E cells, and/or microglia.

Our studies indicate *hey1* and *id2b* are downstream targets of Notch signaling in MG and mediate the effects of Notch signaling on MG's injury-response threshold and proliferation. Hey1 is a member of the basic helix-loop-helix orange family of transcriptional repressors, while Id2b is a helix-loop-helix protein that lacks a DNA binding domain and sequesters basic helix-loop-helix proteins, like Ascl1a, from their target genes. Notch-dependent regulation of MG and MG0-derived progenitor proliferation is similar to what's observed in brain radial glia where Notch signaling maintains neural stem cell quiescence and regulates proliferation of transient amplifying cells (Alunni et al., 2013; Engler, Zhang, & Taylor, 2018; Imayoshi, Sakamoto, Yamaguchi, Mori, & Kageyama, 2010; Kawai et al., 2017; Than-Trong et al., 2018). Furthermore, Hey1 can suppress expression of Ascl1 and Ascl1-regulated genes which is necessary for establishing a transient amplifying population of neural progenitors in the adult brain (Kim, Leung, Reed, & Johnson, 2007; Sakamoto, Hirata, Ohtsuka, Bessho, & Kageyama, 2003). Importantly, Ascl1a is a pioneer transcription factor that can enhance chromatin accessibility across the genome and thereby influencing the expression of many other genes (Wapinski et al., 2017). Thus, the Notch-Hey1-Ascl1a signaling axis identified in zebrafish MG appears to be a conserved pathway in a variety of adult radial glial stem cell populations.

In both zebrafish and mice, Notch signaling is necessary for MG differentiation (Bernardos, Lentz, Wolfe, & Raymond, 2005; Jadhav, Cho, & Cepko, 2006; Nelson et al., 2011; Scheer, Groth, Hans, & Campos-Ortega, 2001). Notch signaling is restricted to MG in the postnatal mouse retina, and here we report it is also restricted to MG in the developing zebrafish retina. However, while the adult zebrafish retina retains relatively high levels of Notch signaling that is regulated by Notch inhibitors and retinal injury, the residual Notch signaling in mouse MG is not regulated by these treatments (Elsaeidi et al., 2018; Nelson et al., 2011). Interestingly, the suppression of Notch signaling during mouse development correlates with the loss of MG stem cell potential (Loffler et al., 2015).

In addition to influencing MG's injury-response threshold, our data supports the idea that Notch signaling inhibition helps maintain MG-derived progenitors in a proliferative state and that the return of Notch signaling around 4 dpi participates in cell cycle exit as progenitors prepare for differentiation. Consistent with this, we previously reported conditional activation of Notch signaling from 3-4 dpi suppressed proliferation of MG-derived progenitors (Wan et al., 2012), and here we report that Notch inhibition from 2-4 dpi stimulated proliferation of MG-derived progenitors. Furthermore, forced

expression of Dll4, Dlb, Notch3, Hey1 or Id2b inhibited proliferation of MG-derived progenitors, while inactivation of these genes enhanced this proliferation. Although overexpression studies are not physiological they are consistent with our gene inactivation experiments. Surprisingly, our conclusions are at odds with those recently reported by Campbell et al., 2021 indicating Notch signaling is necessary for proliferation of MG-derived progenitors. In those studies, MO-mediated gene knockdown was the sole technique used to manipulate Notch signaling.

In addition to their role in retina regeneration, Dll4 and Notch3 are required for angiogenesis and oligodendrocyte development, and loss of either gene is lethal (Leslie et al., 2007; Zaucker, Mercurio, Sternheim, Talbot, & Marlow, 2013). Thus, one may wonder why the *ubi:Cas9*;*u6:dll4-gRNAs*$_{1,2}$ and *ubi:Cas9*;*u6:n3-gRNAs*$_{1,2}$ transgenic fish used in our studies survive to adulthood. We suspect mosaicism in CRISPR-mediated gene editing underlies this survival. This mosaicism may allow normal development to ensue; however, gene edits will continue to accumulate throughout the fish's life, which led to the noted enhanced regeneration phenotype in adult fish. We also note that although many homozygous *notch3* mutant fish do not survive to adulthood, some do (Zaucker et al., 2013).

In summary, our studies reveal a role for Notch signaling in regulating MG's injury-response threshold, licensing MG for proliferation, and regulating the proliferation of MG-derived progenitors. Our analysis of mechanisms underlying these processes identified Hey1 and Id2b that reflect a bifurcation point in MG Notch signaling and distinguishes MG's injury-response threshold from proliferation of MG-derived progenitors. These studies not only further our understanding of how Notch signaling controls retina regeneration in zebrafish, but also suggests that enhancing Notch signaling in mammalian MG may improve their regenerative potential.

References

Alunni, A., Krecsmarik, M., Bosco, A., Galant, S., Pan, L., Moens, C. B., & Bally-Cuif, L. (2013). Notch3 signaling gates cell cycle entry and limits neural stem cell amplification in the adult pallium. *Development, 140*(16), 3335-3347. doi:10.1242/dev.095018

Alvarez, Y., Cederlund, M. L., Cottell, D. C., Bill, B. R., Ekker, S. C., Torres-Vazquez, J., . . . Kennedy, B. N. (2007). Genetic determinants of hyaloid and retinal vasculature in zebrafish. *BMC Dev Biol, 7*, 114. doi:10.1186/1471-213X-7-114

Attwell, D., Buchan, A. M., Charpak, S., Lauritzen, M., Macvicar, B. A., & Newman, E. A. (2010). Glial and neuronal control of brain blood flow. *Nature, 468*(7321), 232-243. doi:10.1038/nature09613

Bernardos, R. L., Lentz, S. I., Wolfe, M. S., & Raymond, P. A. (2005). Notch-Delta signaling is required for spatial patterning and Muller glia differentiation in the zebrafish retina. *Dev Biol, 278*(2), 381-395. doi:10.1016/j.ydbio.2004.11.018

Buenrostro, J. D., Wu, B., Chang, H. Y., & Greenleaf, W. J. (2015). ATAC-seq: A Method for Assaying Chromatin Accessibility Genome-Wide. *Curr Protoc Mol Biol, 109*, 21.29.21-21.29.29. doi:10.1002/0471142727.mb2129s109

Campbell, L. J., Hobgood, J. S., Jia, M., Boyd, P., Hipp, R. I., & Hyde, D. R. (2021). Notch3 and DeltaB maintain Muller glia quiescence and act as negative regulators of regeneration in the light-damaged zebrafish retina. *Glia, 69*, 546-566. doi:10.1002/glia.23912

Conner, C., Ackerman, K. M., Lahne, M., Hobgood, J. S., & Hyde, D. R. (2014). Repressing notch signaling and expressing TNFalpha are sufficient to mimic retinal regeneration by inducing Muller glial proliferation to generate committed progenitor cells. *J Neurocsci, 34*(43), 14403-14419. doi:10.1523/JNEUROSCI.0498-14.2014

Elsaeidi, F., Macpherson, P., Mills, E. A., Jui, J., Flannery, J. G., & Goldman, D. (2018). Notch Suppression Collaborates with Ascl1 and Lin28 to Unleash a Regenerative Response in Fish Retina, But Not in Mice. *J Neurosci, 38*(9), 2246-2261. doi:10.1523/JNEUROSCI.2126-17.2018

Engler, A., Zhang, R., & Taylor, V. (2018). Notch and Neurogenesis. *Adv Exp Med Biol, 1066*, 223-234. doi:10.1007/978-3-319-89512-3_11

Fausett, B. V., & Goldman, D. (2006). A role for alpha1 tubulin-expressing Muller glia in regeneration of the injured zebrafish retina. *J Neurosci, 26*(23), 6303-6313. doi:10.1523/JNEUROSCI.0332-06.2006

Fausett, B. V., Gumerson, J. D., & Goldman, D. (2008). The proneural basic helix-loop-helix gene ascl1a is required for retina regeneration. *J Neurosci, 28*(5), 1109-1117. doi:10.1523/JNEUROSCI.4853-07.2008

Garhofer, G., Chua, J., Tan, B., Wong, D., Schmidl, D., & Schmetterer, L. (2020). Retinal Neurovascular Coupling in Diabetes. *J Clin Med, 9*(9), 2829. doi:10.3390/jcm9092829

Goldman, D. (2014). Muller glial cell reprogramming and retina regeneration. *Nature reviews. Neuroscience, 15*(7), 431-442. doi:10.1038/nrn3723

Gorsuch, R. A., Lahne, M., Yarka, C. E., Petravick, M. E., Li, J., & Hyde, D. R. (2017). Sox2 regulates Muller glia reprogramming and proliferation in the regenerating zebrafish retina via Lin28 and Ascl1a. *Exp Eye Res, 161*, 174-192. doi:10.1016/j.exer.2017.05.012

Hoang, T., Wang, J., Boyd, P., Wang, F., Santiago, C., Jiang, L., . . . Blackshaw, S. (2020). Gene regulatory networks controlling vertebrate retinal regeneration. *Science, 370*(6519), eabb8598. doi:10.1126/science.abb8598

Hwang, W. Y., Fu, Y., Reyon, D., Maeder, M. L., Tsai, S. Q., Sander, J. D., . . . Joung, J. K. (2013). Efficient genome editing in zebrafish using a CRISPR-Cas system. *Nat Biotechnol, 31*(3), 227-229. doi:10.1038/nbt.2501

Imayoshi, I., Sakamoto, M., Yamaguchi, M., Mori, K., & Kageyama, R. (2010). Essential roles of Notch signaling in maintenance of neural stem cells in developing and adult brains. *J Neurosci, 30*(9), 3489-3498. doi:10.1523/JNEUROSCI.4987-09.2010

Iribarne, M., Hyde, D. R., & Masai, I. (2019). TNFalpha Induces Muller Glia to Transition From Non-proliferative Gliosis to a Regenerative Response in Mutant Zebrafish Presenting Chronic Photoreceptor Degeneration. *Front Cell Dev Biol, 7*, 296. doi:10.3389/fcell.2019.00296

Ivanova, E., Alam, N. M., Prusky, G. T., & Sagdullaev, B. T. (2019). Blood-retina barrier failure and vision loss in neuron-specific degeneration. *JCI Insight, 4*, e126747. doi:10.1172/jci.insight.126747

Jadhav, A. P., Cho, S. H., & Cepko, C. L. (2006). Notch activity permits retinal cells to progress through multiple progenitor states and acquire a stem cell property. *Proc Natl Acad Sci U S A, 103*(50), 18998-19003. doi:10.1073/pnas.0608155103

Johnson, K., Barragan, J., Bashiruddin, S., Smith, C. J., Tyrrell, C., Parsons, M. J., . . . Barresi, M. J. (2016). Gfap-positive radial glial cells are an essential progenitor population for later-born neurons and glia in the zebrafish spinal cord. *Glia, 64*(7), 1170-1189. doi:10.1002/glia.22990

Kassen, S. C., Ramanan, V., Montgomery, J. E., C, T. B., Liu, C. G., Vihtelic, T. S., & Hyde, D. R. (2007). Time course analysis of gene expression during light-induced photoreceptor cell death and regeneration in albino zebrafish. *Dev Neurobiol, 67*(8), 1009-1031. doi:10.1002/dneu.20362

Kawai, H., Kawaguchi, D., Kuebrich, B. D., Kitamoto, T., Yamaguchi, M., Gotoh, Y., & Furutachi, S. (2017). Area-Specific Regulation of Quiescent Neural Stem Cells by Notch3 in the Adult Mouse Subependymal Zone. *J Neurosci, 37*(49), 11867-11880. doi:10.1523/JNEUROSCI.0001-17.2017

Kim, E. J., Leung, C. T., Reed, R. R., & Johnson, J. E. (2007). In vivo analysis of Ascl1 defined progenitors reveals distinct developmental dynamics during adult neurogenesis and gliogenesis. *J Neurosci, 27*(47), 12764-12774. doi:10.1523/JNEUROSCI.3178-07.2007

Lahne, M., Nagashima, M., Hyde, D. R., & Hitchcock, P. F. (2020). Reprogramming Muller Glia to Regenerate Retinal Neurons. *Annu Rev Vis Sci, 6*, 171-193. doi:10.1146/annurev-vision-121219-081808

Lee, M. S., Wan, J., & Goldman, D. (2020). Tgfb3 collaborates with PP2A and notch signaling pathways to inhibit retina regeneration. *Elife, 9*, e55137. doi:10.7554/eLife.55137

Lenkowski, J. R., & Raymond, P. A. (2014). Muller glia: Stem cells for generation and regeneration of retinal neurons in teleost fish. *Progress in retinal and eye research, 40*, 94-123. doi:10.1016/j.preteyeres.2013.12.007

Leslie, J. D., Ariza-McNaughton, L., Bermange, A. L., McAdow, R., Johnson, S. L., & Lewis, J. (2007). Endothelial signalling by the Notch ligand Delta-like 4 restricts angiogenesis. *Development, 134*(5), 839-844. doi:10.1242/dev.003244

Lessieur, E. M., Song, P., Nivar, G. C., Piccillo, E. M., Fogerty, J., Rozic, R., & Perkins, B. D. (2019). Ciliary genes arl13b, ahi1 and cc2d2a differentially modify expression of visual acuity phenotypes but do not enhance retinal degeneration due to mutation of cep290 in zebrafish. *PLoS One, 14*(4), e0213960. doi:10.1371/journal.pone.0213960

Loffler, K., Schafer, P., Volkner, M., Holdt, T., & Karl, M. O. (2015). Age-dependent Muller glia neurogenic competence in the mouse retina. *Glia, 63*, 1809-1824. doi:10.1002/glia.22846

MacDonald, R. B., Randlett, O., Oswald, J., Yoshimatsu, T., Franze, K., & Harris, W. A. (2015). Muller glia provide essential tensile strength to the developing retina. *J Cell Biol, 210*(7), 1075-1083. doi:10.1083/jcb.201503115

Maillard, I., Tu, L., Sambandam, A., Yashiro-Ohtani, Y., Millholland, J., Keeshan, K., . . . Pear, W. S. (2006). The requirement for Notch signaling at the beta-selection checkpoint in vivo is absolute and independent of the pre-T cell receptor. *J Exp Med, 203*(10), 2239-2245. doi:10.1084/jem.20061020

Maillard, I., Weng, A. P., Carpenter, A. C., Rodriguez, C. G., Sai, H., Xu, L., . . . Pear, W. S. (2004). Mastermind critically regulates Notch-mediated lymphoid cell fate decisions. *Blood, 104*(6), 1696-1702. doi:10.1182/blood-2004-02-0514

Montgomery, J. E., Parsons, M. J., & Hyde, D. R. (2010). A novel model of retinal ablation demonstrates that the extent of rod cell death regulates the origin of the regenerated zebrafish rod photoreceptors. *J Comp Neurol, 518*(6), 800-814. doi:10.1002/cne.22243

Moreno-Mateos, M. A., Vejnar, C. E., Beaudoin, J. D., Fernandez, J. P., Mis, E. K., Khokha, M. K., & Giraldez, A. J. (2015). CRISPRscan: designing highly efficient sgRNAs for CRISPR-Cas9 targeting in vivo. *Nat Methods, 12*(10), 982-988. doi:10.1038/nmeth.3543

Nagashima, M., Barthel, L. K., & Raymond, P. A. (2013). A self-renewing division of zebrafish Muller glial cells generates neuronal progenitors that require N-cadherin to regenerate retinal neurons. *Development, 140*(22), 4510-4521. doi:10.1242/dev.090738

Nam, Y., Sliz, P., Song, L., Aster, J. C., & Blacklow, S. C. (2006). Structural basis for cooperativity in recruitment of MAML coactivators to Notch transcription complexes. *Cell, 124*(5), 973-983. doi:10.1016/j.cell.2005.12.037

Nelson, B. R., Ueki, Y., Reardon, S., Karl, M. O., Georgi, S., Hartman, B. H., . . . Reh, T. A. (2011). Genome-wide analysis of Muller glial differentiation reveals a requirement for Notch signaling in postmitotic cells to maintain the glial fate. *PLoS One, 6*(8), e22817. doi:10.1371/journal.pone.0022817

Parsons, M. J., Pisharath, H., Yusuff, S., Moore, J. C., Siekmann, A. F., Lawson, N., & Leach, S. D. (2009). Notch-responsive cells initiate the secondary transition in larval zebrafish pancreas. *Mech Dev, 126*(10), 898-912. doi:10.1016/j.mod.2009.07.002

Powell, C., Grant, A. R., Cornblath, E., & Goldman, D. (2013). Analysis of DNA methylation reveals a partial reprogramming of the Muller glia genome during retina regeneration. *Proc Natl Acad Sci U S A, 110*(49), 19814-19819. doi:10.1073/pnas.1312009110

Ramachandran, R., Fausett, B. V., & Goldman, D. (2010a). Ascl1a regulates Muller glia dedifferentiation and retinal regeneration through a Lin-28-dependent, let-7 microRNA signalling pathway. *Nat Cell Biol, 12*(11), 1101-1107. doi:10.1038/ncb2115

Ramachandran, R., Reifler, A., Parent, J.M and Goldman, D. (2010). Conditional gene expression and lineage tracing of tuba1a expressing cells during zebrafish development and retina regeneration. *J Comp Neurol, 518*(20), 4196-4212. doi: 10.1002/cne.22448

Ramachandran, R., Zhao, X. F., & Goldman, D. (2011). Ascl1a/Dkk/{beta}-catenin signaling pathway is necessary and glycogen synthase kinase-3{beta} inhibition is sufficient for zebrafish retina regeneration. *Proc Natl Acad Sci U S A, 108*, 15858-15863. doi:10.1073/pnas.1107220108

Ramachandran, R., Zhao, X. F., & Goldman, D. (2012). Insm1a-mediated gene repression is essential for the formation and differentiation of Muller glia-derived progenitors in the injured retina. *Nat Cell Biol, 14*(10), 1013-1023. doi:10.1038/ncb2586

Reichenbach, A., & Bringmann, A. (2013). New functions of Muller cells. *Glia, 61*(5), 651-678. doi:10.1002/glia.22477

Riesenberg, A. N., Conley, K. W., Le, T. T., & Brown, N. L. (2018). Separate and coincident expression of Hes1 and Hes5 in the developing mouse eye. *Dev Dyn, 247*(1), 212-221. doi:10.1002/dvdy.24542

Sakamoto, M., Hirata, H., Ohtsuka, T., Bessho, Y., & Kageyama, R. (2003). The basic helix-loop-helix genes Hesr1/Hey1 and Hesr2/Hey2 regulate maintenance of neural precursor cells in the brain. *J Biol Chem, 278*(45), 44808-44815. doi:10.1074/jbc.M300448200

Scheer, N., Groth, A., Hans, S., & Campos-Ortega, J. A. (2001). An instructive function for Notch in promoting gliogenesis in the zebrafish retina. *Development, 128*(7), 1099-1107.

Sentmanat, M. F., Peters, S. T., Florian, C. P., Connelly, J. P., & Pruett-Miller, S. M. (2018). A Survey of Validation Strategies for CRISPR-Cas9 Editing. *Sci Rep, 8*(1), 888. doi:10.1038/s41598-018-19441-8

Sifuentes, C. J., Kim, J. W., Swaroop, A., & Raymond, P. A. (2016). Rapid, Dynamic Activation of Muller Glial Stem Cell Responses in Zebrafish. *Invest Ophthalmol Vis Sci, 57*(13), 5148-5160. doi:10.1167/iovs.16-19973

Than-Trong, E., Ortica-Gatti, S., Mella, S., Nepal, C., Alunni, A., & Bally-Cuif, L. (2018). Neural stem cell quiescence and stemness are molecularly distinct outputs of the Notch3 signalling cascade in the vertebrate adult brain. *Development, 145*(10), dev161034. doi:10.1242/dev.161034

Vejnar, C. E., Moreno-Mateos, M. A., Cifuentes, D., Bazzini, A. A., & Giraldez, A. J. (2016). Optimized CRISPR-Cas9 System for Genome Editing in Zebrafish. *Cold Spring Harb Protoc, 2016*(10), doi:10.1101/pdb.prot086850. doi:10.1101/pdb.prot086850

Wan, J., & Goldman, D. (2016). Retina regeneration in zebrafish. *Curr Opin Genet Dev, 40*, 41-47. doi:10.1016/j.gde.2016.05.009

Wan, J., & Goldman, D. (2017). Opposing Actions of Fgf8a on Notch Signaling Distinguish Two Muller Glial Cell Populations that Contribute to Retina Growth and Regeneration. *Cell Rep, 19*(4), 849-862. doi:10.1016/j.celrep.2017.04.009

Wan, J., Ramachandran, R., & Goldman, D. (2012). HB-EGF is necessary and sufficient for Muller glia dedifferentiation and retina regeneration. *Dev Cell, 22*(2), 334-347. doi:10.1016/j.devcel.2011.11.020

Wan, J., Zhao, X. F., Vojtek, A., & Goldman, D. (2014). Retinal Injury, Growth Factors, and Cytokines Converge on beta-Catenin and pStat3 Signaling to Stimulate Retina Regeneration. *Cell Reports, 9*, 285-297. doi:10.1016/j.celrep.2014.08.048

Wapinski, O. L., Lee, Q. Y., Chen, A. C., Li, R., Corces, M. R., Ang, C. E., . . . Chang, H. Y. (2017). Rapid Chromatin Switch in the Direct Reprogramming of Fibroblasts to Neurons. *Cell Rep, 20*(13), 3236-3247. doi:10.1016/j.celrep.2017.09.011

Xia, W. (2019). gamma-Secretase and its modulators: Twenty years and beyond. *Neurosci Lett, 701*, 162-169. doi:10.1016/j.neulet.2019.02.011

Yin, L., Maddison, L. A., Li, M., Kara, N., LaFave, M. C., Varshney, G. K., . . . Chen, W. (2015). Multiplex Conditional Mutagenesis Using Transgenic Expression of Cas9 and sgRNAs. *Genetics, 200*(2), 431-441. doi:10.1534/genetics.115.176917

Zaucker, A., Mercurio, S., Sternheim, N., Talbot, W. S., & Marlow, F. L. (2013). notch3 is essential for oligodendrocyte development and vascular integrity in zebrafish. *Dis Model Mech, 6*(5), 1246-1259. doi:10.1242/dmm.012005

Zhao, L., Borikova, A. L., Ben-Yair, R., Guner-Ataman, B., MacRae, C. A., Lee, R. T., . . . Burns, C. E. (2014). Notch signaling regulates cardiomyocyte proliferation during zebrafish heart regeneration. *Proc Natl Acad Sci U S A, 111*(4), 1403-1408. doi:10.1073/pnas.1311705111

Zhao, X. F., Wan, J., Powell, C., Ramachandran, R., Myers, M. G., Jr., & Goldman, D. (2014). Leptin and IL-6 Family Cytokines Synergize to Stimulate Muller Glia Reprogramming and Retina Regeneration. *Cell Reports, 9*, 272-284. doi:10.1016/j.celrep.2014.08.047

Data accessibility citation

Goldman, D. (2021) https://www.ncbi.nlm.nih.gov/geo/query/acc.cgi?acc=GSE160179.

Author contributions

AS designed and performed all experiments except ATACseq and generation of CRISPR gene edited fish. SD performed ATACseq experiments and generated CRISPR gene edited fish. JJ analyzed bulk RNAseq and scRNAseq data and helped in transfections. DG conceived, designed, and supervised the work and co-wrote the manuscript and helped generate transgenic fish. All authors reviewed and edited the manuscript.

Figure legends

Figure 1: Notch signaling in the developing retina. A, GFP and mCherry immunofluorescence on retinal sections from *tp1:mCherry;gfap:GFP* transgenic fish at different times post fertilization. Dashed oval identifies retinal periphery where retinal stem cells involved in retinal expansion reside. **B**, PCR and agarose gel analysis of *mCherry* RNA expression in developing *tp1:mCherry* fish. **C**, qPCR analysis of *mCherry* RNA expression in retinas of developing *tp1:mCherry* fish. Compared to 2 dpf, **P*=0.0252 (5dpf), ***P*=0.0076 (7dpf), **P*=0.0122 (15dpf), ***P*=0.0065 (1mpf), ***P*=0.0074 (2mpf), ***P*=0.0016 (4mpf), ****P*=0.0008 (6mpf). **D**, GFP and mCherry immunofluorescence on adult retinal sections from *tp1:mCherry;gfap:GFP* transgenic fish. **E**, Representative fluorescent image of mCherry immunofluorescence (red) and EdU Click-iT chemistry (green) on retinal sections at 2 and 4 dpi. Arrowheads point to EdU+/mCherry- MG-derived progenitors. **F**, Graph is qPCR quantification of *mCherry* RNA expression in adult retina of *tp1:mCherry* fish at various times post needle poke injury. Compared to 0 dpi, **P*=0.0478 at 0.5 and 2 days post injury. **G**, PCR and agarose gel analysis of *mCherry* and $gapdh_s$ RNA expression in adult *tp1:mCherry* fish treated +/-DAPT. Abbreviations: d, days; m, months; ONL, outer nuclear layer; INL, inner nuclear layer. Scale bar is 100 μm.

Figure 2: Injury-dependent regulation of MG gene expression and chromatin accessibility. A, MA plot of RNAseq data using MG purified from uninjured and injured fish retinas. **B**, qPCR analysis of select injury-regulated genes. Compared to uninjured control samples, induced genes at all times post injury ***P*<0.001. For all repressed genes at 12 hours post injury ***P*<0.003; for repressed genes at 24 hours post injury ***P*<0.001 for *hey1* and *id2b*, *P*=0.06 for *pdlim2*; for repressed genes at 48 hours post injury ***P*<0.008 for *hey1* and *id2b*, *P*=0.053 for *pdlim2*; for repressed genes at 96 hours post injury **P*<0.014 for *hey1* and *id2b*, *P*=0.79 for *pdlim2* at 96 hours post injury **C**, Volcano plot of ATACseq data using MG purified from uninjured and injured fish retinas. **D**, Intersection of regeneration-associated genes with those whose chromatin accessibility changes with injury.

Figure 3: Notch-dependent regulation of MG gene expression and chromatin accessibility in uninjured retina. A, MA plot of RNAseq data from MG of uninjured fish treated +/- DAPT. **B**, Intersection of regeneration-associated genes with DAPT-regulated genes. Proportional Venn diagram illustrating intersection of gene lists. Note circles outside of main Venn diagram report the number of genes either induced or suppressed (indicated by arrow direction) in the main Venn diagram. **C**, Volcano plot of ATACseq data from MG of uninjured fish treated +/- DAPT. **D**, Intersection of regeneration-associated genes with those whose chromatin accessibility changes with DAPT treatment.

Figure 4: Hey1 and Id2b regulate MG's regenerative response. A, Illustration of *hey1* gene promoter from human, mouse and zebrafish with Rbpj binding sites indicated. **B**, Luciferase assays for Notch (NICD) dependent activation of Wt and mutant *hey1* promoter activity; Compared to Wt alone, ***P<0.0001. **C**, **F**, EdU Click-iT chemistry on retinal sections identifies proliferating cells in Wt fish treated with indicated MOs (**C**) or Cas9 and indicated gRNAs (**F**). **D**, **G**, **I**, Quantification of the number of EdU+ cells at 4 dpi; (**D**)***P=0.0008, (**G**) ***P<0.0001, (**I**) ***P<0.0001. **E**, **H**, Quantification of the width of the proliferative zone in retinas at 4 dpi; (**E**) ***P<0.0001, (**H**) ***P=0.0004. **J**, PCR analysis of the effects Hey1 expression has on injury-dependent induction of *ascl1a* and *lin28a*. Abbreviations: MO, morpholino; C-MO or Con-MO, control-MO; ONL, outer nuclear layer; INL, inner nuclear layer; GCL, ganglion cell layer; Wt, wild type; m, mutant. Scale bars are 100 μm.

Figure 5: Analysis of Notch ligand and receptor gene expression in the uninjured and injured zebrafish retina. A, Expression level of indicated RNAs based on bulk RNAseq data generated from GFP+ MG FACS purified from uninjured *gfap:GFP* and GFP+ activated MG and MG-derived progenitors FACS purified from injured (2 dpi) *1016 tuba1a:GFP* fish. **B**, qPCR heat map illustrating temporal changes in the expression of Notch ligand and receptor encoding genes at various times post needle poke injury. Compared to uninjured control, *dla*, **P<0.004 at 6hpi and 4dpi; *dlb*, *P<0.04 at 6hpi, 1dpi, 4dpi, and 7dpi; *dlc*, *P<0.03 at 6hpi and 7dpi, **P<0.005 at 4dpi; *dld*, **P<0.004 at 6hpi, 2dpi, and 4dpi, *P<0.03 at

7dpi; dll4, **P<0.002 at 6hpi, 14hpi, 1dpi, and 2dpi; *j1a*, *P<0.05 at 6hpi and 1dpi, **P<0.005 at 4dpi; *j1b*, *P<0.05 at 4dpi; *j2a*, *P<0.016 at 6hpi and 4dpi, **P<0.005 at 2dpi, and *P<0.05 at 7dpi; *j2b*, *P<0.05 at 6hpi and 4dpi; *n1a*, *P<0.05 at 1-7dpi; *n1b*, **P<0.0018 at 2dpi, *P<0.05 at 4 and 7dpi; *n2*, *P<0.05 at 6hpi, 1dpi, and 4dpi, ***P<0.0005 at 2dpi; *n3*, ***P<0.0001 at 6hpi, **P<0.006 at 14hpi, and 1dpi, *P<0.05 at 2-7dpi. **C**, Expression level of indicated RNAs in MG and nonMG based on bulk RNAseq data generated by Hoang et al., 2020 using GFP+ MG and GFP- nonMG FACS purified from uninjured *gfap:GFP* fish. **D**, Temporal changes in indicated genes at various times post light damage based on bulk RNAseq data generated by Hoang et al., 2020, using GFP+ MG and GFP- nonMG FACS purified from injured *gfap:GFP* fish. **E**, Dot plot visualization of *dlb*, *dll4* and *notch3* gene expression across retinal cell types in the uninjured and NMDA injured retina based on scRNAseq data from Hoang et al., 2020. These data, along with that for control genes and the number of cells with detectable expression, is shown in Figure S4C. Abbreviations: *j*, *jag*; *n*, *notch*; hpi, hours post injury; dpi, days post injury; FPKM, Fragments Per Kilobase of transcript per Million mapped reads; peri, pericyte; RPE, retinal pigment epithelium; HC, horizontal cell; V/E, vascular endothelial cell; Mic, microglia; RGC, retinal ganglion cell; Gly-AC, glycinergic amacrine cell; GAB-AC, GABAergic amacrine cell; BC, bipolar cell; C-BC, cone bipolar cell; Prog, progenitors in the ciliary margin; ActMG, activated MG.

Figure 6: Dll4 regulates MG's injury response threshold and proliferation of MG-derived progenitors. **A**, Diagram of the *dll4* gene with MO and gRNA target sites indicated. **B, F, J,** Fluorescent images showing EdU Click-iT chemistry on retinal sections at 4 dpi. **C, G, K,** Quantification of the number of EdU+ cells at 4 dpi; (**C**), compared to C-MO**P=0.0351 (0.2mM), **P=0.0022 (0.5mM), ***P=0.0003 (1mM); (**G**), compared to Cas9 ***P<0.0001; (**K**), ***P<0.0001. **D, H, L,** Quantification of the width of the proliferative zone in retinas at 4 dpi; (**D**), ***P<0.0001; (**H**), ***P<0.0001; (**L**), ***P<0.0001. **E, I, M,** Quantification of TUNEL+ cells at 1 dpi. Abbreviations: Wt, wild type; MO, morpholino; C-MO or Con-

MO, control-MO; ONL, outer nuclear layer; INL, inner nuclear layer; GCL, ganglion cell layer. Scale bars are 100 μm.

Figure 7: Dll4 and Dlb engage the Notch3 receptor to induce Hey1 and Id2b expression and control retina regeneration. A, C, Quantification of proliferating MG-derived progenitors at a needle poke injury site (2 dpi). **B**, **D**, Quantification of the zone of proliferating MG at a needle poke injury site (2 dpi). (**A**), Compared to (C-MO, Wt), ***P*=0.0014 (C-MO, Dll4); **P*=0.0218 (C-MO, Dlb); ***P*=0.0031 (notch3-MO, Wt); **P*=0.0197 (notch3-MO, Dll4); **P*=0.0394 (notch3-MO, Dlb). (**B**), Compared to (C-MO, Wt), ****P*=0.0003 C-MO, Dll4); ***P*=0.0011 (C-MO, Dlb); ****P*<0.0001 (notch3-MO, Wt); ****P*=0.0009 (notch3-MO, Dll4); ***P*=0.0022 (notch3-MO, Dlb). (**C**), Compared to control MO (Con) in Wt retina, ****P*<0.0001 (Wt, dll4-MO); ***P*=0.0056 (Wt, dlb-MO); ****P*<0.0001 (Wt, n3-MO); ***P*=0.0042 (Hey1, Con-MO); **P*=0.0228 (Hey1, dll4-MO); **P*=0.0132 (Hey1, dlb-MO); ***P*=0.0025 (Hey1, n3-MO); ****P*=0.0004 (Id2b, dll4-MO); **P*=0.021 (Id2b, dlb-MO); ****P*=0.0002 (Id2b, n3-MO). (**D**), Compared to control MO (Con) in Wt retina, ****P*<0.0001 (Wt, dll4-MO); ****P*=0.0003 (Wt, dlb-MO); ****P*<0.0001 (Wt, n3-MO); ****P*=0.0003 (Hey1, Con-MO); ****P*<0.0001 (Hey1, dll4-MO); ****P*=0.0001 (Hey1, dlb-MO); ****P*=0.0001 (Hey1, n3-MO); **P*=0.0348 (Id2b, Con-MO); ****P*=0.0006 (Id2b, dl4-MO); ***P*=0.0027 (Id2b, dlb-MO); ****P*<0.0001 (Id2b, n3-MO). Abbreviations: Wt, wild type fish; MO, morpholino; C-MO or con, control MO; n3, notch3; ns, not significant.

Figure 8: Notch signaling in the developing retina. A and **B**, Model illustrating the impact Notch signaling has on MG's regenerative response. **A,** Illustration of the effect of Notch signaling on MG gene expression and chromatin accessibility. Potential retinal cell sources of Dll4 and Dlb are listed. **B**, Illustration of the effect Notch signaling has on MG's threshold response to injury-derived factors. Abbreviations: ONL, outer nuclear layer; INL, inner nuclear layer; GCL, ganglion cell layer. Scale bar is 50

μm. Abbreviations: ONL, outer nuclear layer; INL, inner nuclear layer; GCL, ganglion cell layer; dpf, day post fertilization.

SUPPLEMENTARY FIGURE LEGENDS

Figure S1: Injury-regulated genes and chromatin accessibility. A, PCR and agarose gel analysis of select regeneration-associated genes at various times post injury. **B**, Annotation of injury-regulated ATACseq data to different genic features. **C**, Select ATACseq genomic tracts generated from GFP+ MG FACS purified from uninjured and needle poke injured *gfap:GFP* retinas.

Figure S2: Notch-regulated genes and chromatin accessibility. A, Top 20 injury-responsive genes that are also regulated in a similar direction by DAPT-treatment. **B**, qPCR time course analysis of select DAPT-regulated genes in the uninjured retina. **C**, Annotation of DAPT-regulated ATACseq data to different genic features. **D**, Select ATACseq genomic tracts using GFP+ MG purified from uninjured *gfap:GFP* retinas treated +/-DAPT. **E**, Volcano plot of MG RNAseq data from *gfap:mCherry* and *gfap:mCherrry;hsp70:DN-MAML* heat shock treated fish.

Figure S3: Hey1 and Id2b regulate retina regeneration. A, Illustration of *hey1* and *id2b* genomic DNA with MO and gRNA target sites indicated. **B**, PCR analysis of *hey1*-MO treatment stimulating *hey1* intron retention. **C**, *id2b*-MO suppressed *id2b-GFP* chimeric RNA expression in zebrafish embryos. Numbers in panels refer to number of lissamine+ fish with GFP+ phenotype. **D**, Quantification of EdU+ cells using Click-iT chemistry in *hey1*-MO treated retina; ***P*=0.0054 (0.2mM); ****P*=0.0002 (0.5mM); ****P*=0.0008 (1.0mM). **E**, **F**, Single cell embryos were injected with Cas9 RNA and the indicated gRNAs and raised to adults. Shown is PCR analysis of genomic DNA from fin clips of adult fish. **G**, **H**, Quantification of TUNEL+ cells in the injured retina.

Figure S4: Injury-dependent changes in Notch ligand and receptor gene expression. A, Total retinal RNA was used for PCR analysis of Notch ligand and receptor gene expression at various times post injury. **B**, Percentage of indicated retinal cell type expressing the indicated gene based on data from Hoang et al., 2020. **C**, Dot plot visualization of gene expression across retinal cell types in the uninjured and NMDA injured retina based on scRNAseq data from Hoang et al., 2020. Numbers in parenthesis indicate the number of a particular cell type detected in the sample at each time point. **D**, Experimental time line and representative fluorescent images following DAPT treatment from 2-4 dpi in the needle pole injured retina (EdU+ cells are green and BrdU+ cells are red). Arrows point to double labelled cells. Graph shows percentage of EdU+ cells that are also BrdU+. Abbreviations: *j*, *jag*; *n*, *notch*; hpi, hours post injury; dpi, days post injury; FPKM, Fragments Per Kilobase of transcript per Million mapped reads; peri, pericyte; RPE, retinal pigment epithelium; HC, horizontal cell; V/E, vascular endothelial cell; Mic, microglia; RGC, retinal ganglion cell; Gly-AC, glycinergic amacrine cell; GAB-AC, GABAergic amacrine cell; BC, bipolar cell; C-BC, cone bipolar cell; Prog, progenitors in the ciliary margin; ActMG, activated MG. Scale bar is 100 μm.

Figure S5: Notch ligand encoding genes that regulate MG's injury response. A, *dlb*-MO suppresses *dlb-GFP* chimeric RNA expression in embryos. Numbers in panels refer to number of lissamine+ fish with GFP+ phenotype. **B**, Experimental time line and EdU Click-iT chemistry on retinal sections to detect proliferating cells. **C**, Quantification of EdU+ cells in control and Dlb knockdown retinas; **P*<0.0446. **D**, Quantification of the proliferative zone in the injured retina treated with control and *dlb*-MO; ****P*<0.0001. **E**, PCR analysis of *dll4* RNA expression in retinas treated with control and *dlb*-MO. **F**, Experimental time line and EdU Click-iT chemistry on retinal sections to identify proliferating cells. **G**, Quantification of EdU+ cells in control (Wt) and Dlb overexpressing (Dlb) transgenic fish; ***P*=0.0018. **H**, PCR shows *dll4*-MO stimulates intron retention in the *dll4* RNA. **I**, CRISPR-based gene editing detected in genomic DNA from *ubi:Cas9;u6:dll4gRNA*$_{1,2}$ transgenic fish. **J**, qPCR analysis of *dll4* transgene induction

in *hsp70:dll4-p2A-GFP* fish after heat shock. Abbreviations: MO, morpholino; C-MO or Con-MO, control-MO; n3-MO, notch3-MO; ONL, outer nuclear layer; INL, inner nuclear layer; GCL, ganglion cell layer. Scale bars are 100 μm.

Figure S6: Notch3 regulates MG's threshold response to injury. **A**, Diagram of the *notch3* gene with MO and gRNA target sites indicated. **B**, *notch3*-MO suppresses *notch3-GFP* chimeric RNA expression in embryos. Numbers in panels refer to number of lissamine+ fish with GFP+ phenotype. **C**, **H**, EdU Click-iT assay on retinal sections at 4 dpi to detect proliferating cells. **D**, **I**, Quantification of the number of EdU+ cells at 4 dpi; (**D**) Compared to C-MO, ***P*=0.0019 (0.2mM), ***P*=0.0015 (0.5mM), ****P*=0.0006 (1mM); (**I**) compared to Cas9 ****P*=0.0002. **E**, **J**, Quantification of the width of the proliferative zone in retinas at 4 dpi; (**E**) ****P*<0.0001; (**J**) ****P*<0.0001; **F**, **K**, Quantification of TUNEL+ cells at 1 dpi. **G**, CRISPR-based gene editing detected by PCR using genomic DNA from transgenic fish. Abbreviations: MO, morpholino; C-MO or Con-MO, control-MO; n3-MO, notch3-MO; ONL, outer nuclear layer; INL, inner nuclear layer; GCL, ganglion cell layer. Scale bars are 100 μm.

Supplementary Tables

Table S1: Inj reg genes & chromatin accessibility. Related to Figure 2.

Table S2: Inj reg ATAC genes, promoters, & 1-5kb regions. Related to Figure 2.

Table S3: Inj and DAPT coordinately regulated genes. Related to Figure 3.

Table S4: DAPT & inj regulated ATACseq. Related to Figure 3.

Table S5: DAPT & DN-MAML intersection with regeneration-associated genes. Related to Figure 3.

Table S6: PCR heat map data. Related to Figure 5.

Table S7: Primer, MO, gRNA list. Related to Material and methods.

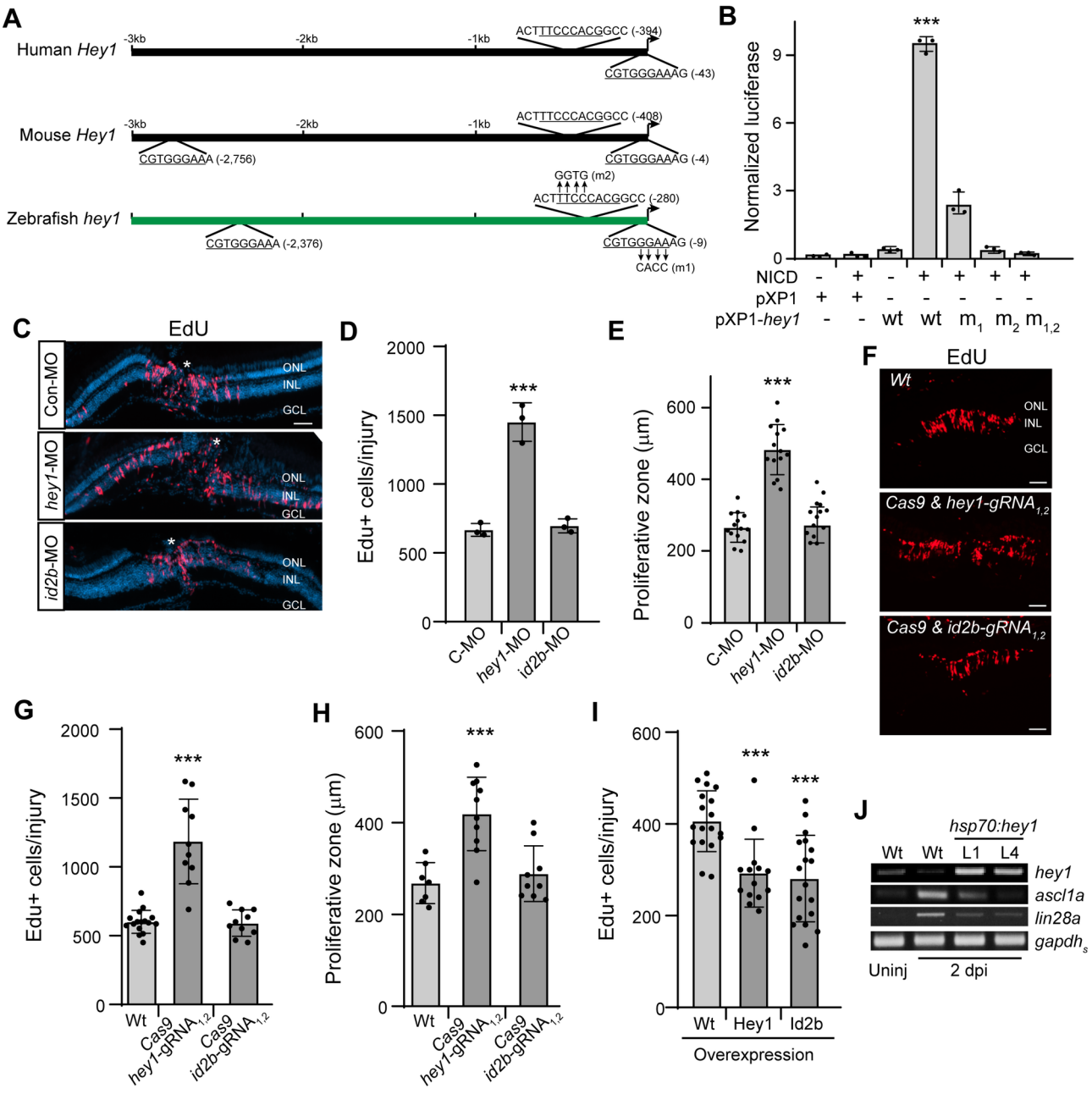

GLIA_24075_Figure 4dg.tif

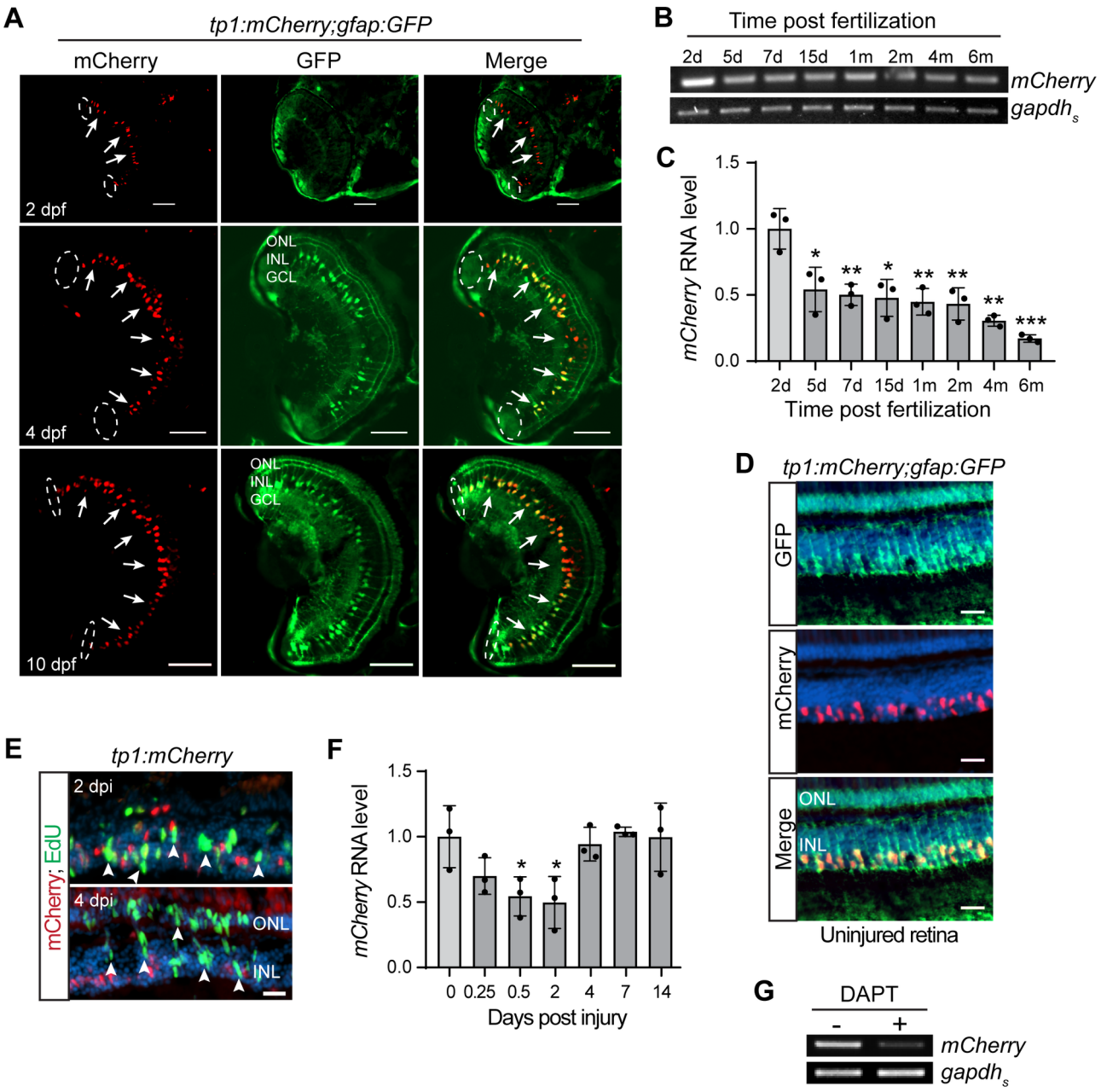

GLIA_24075_Figure_1dg_revised.tif

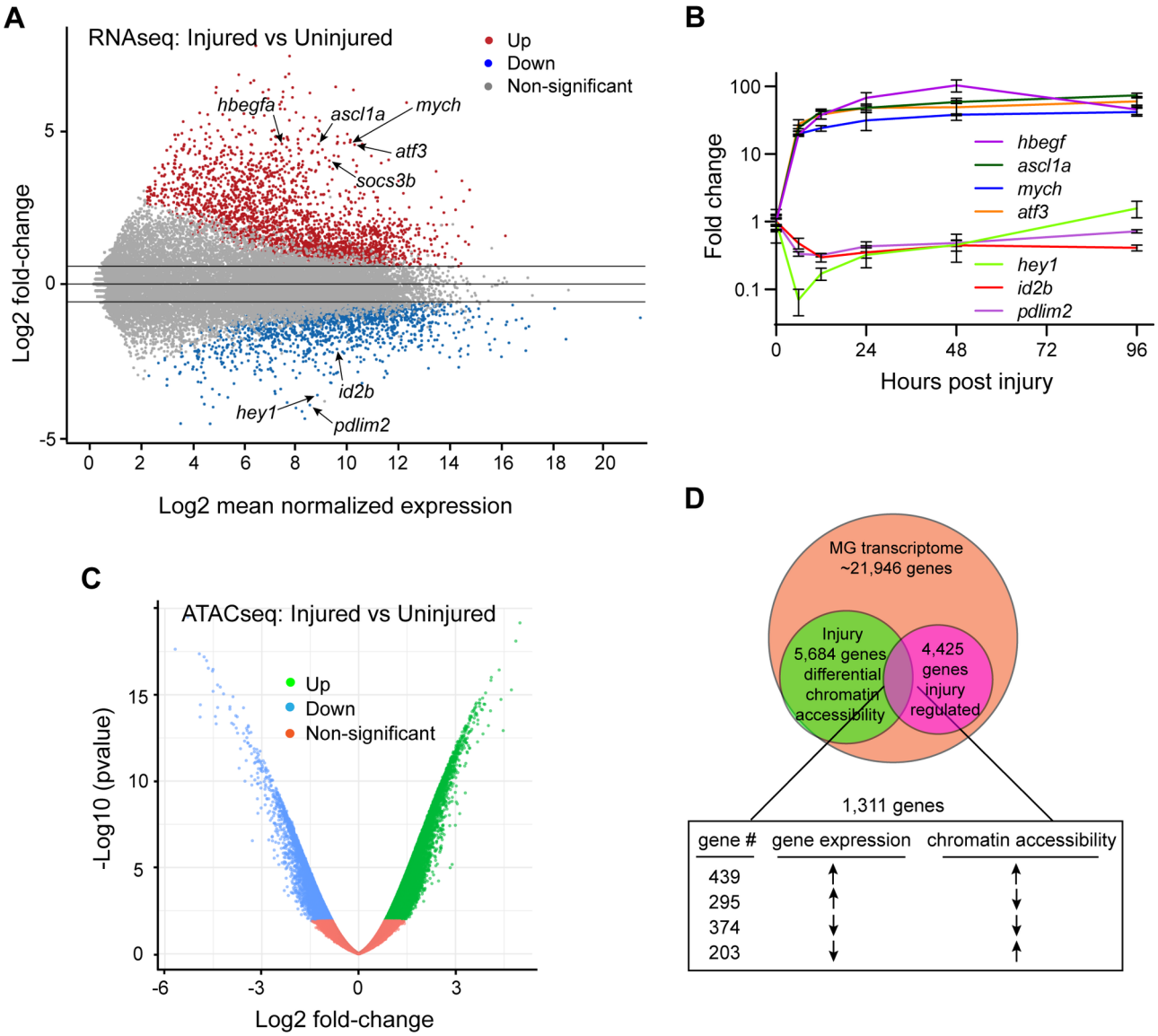

GLIA_24075_Figure_2.tif

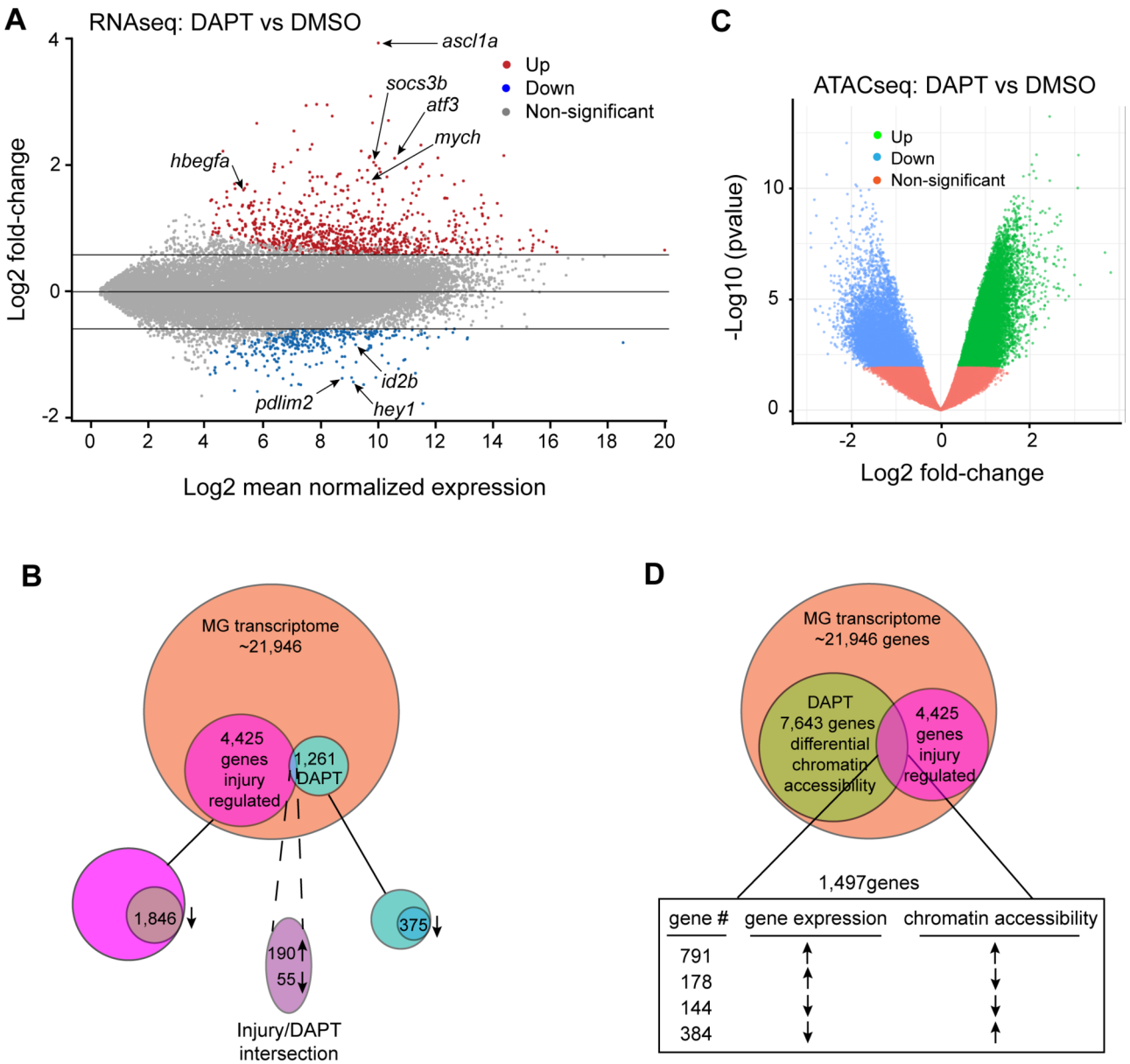

GLIA_24075_Figure_3.tif

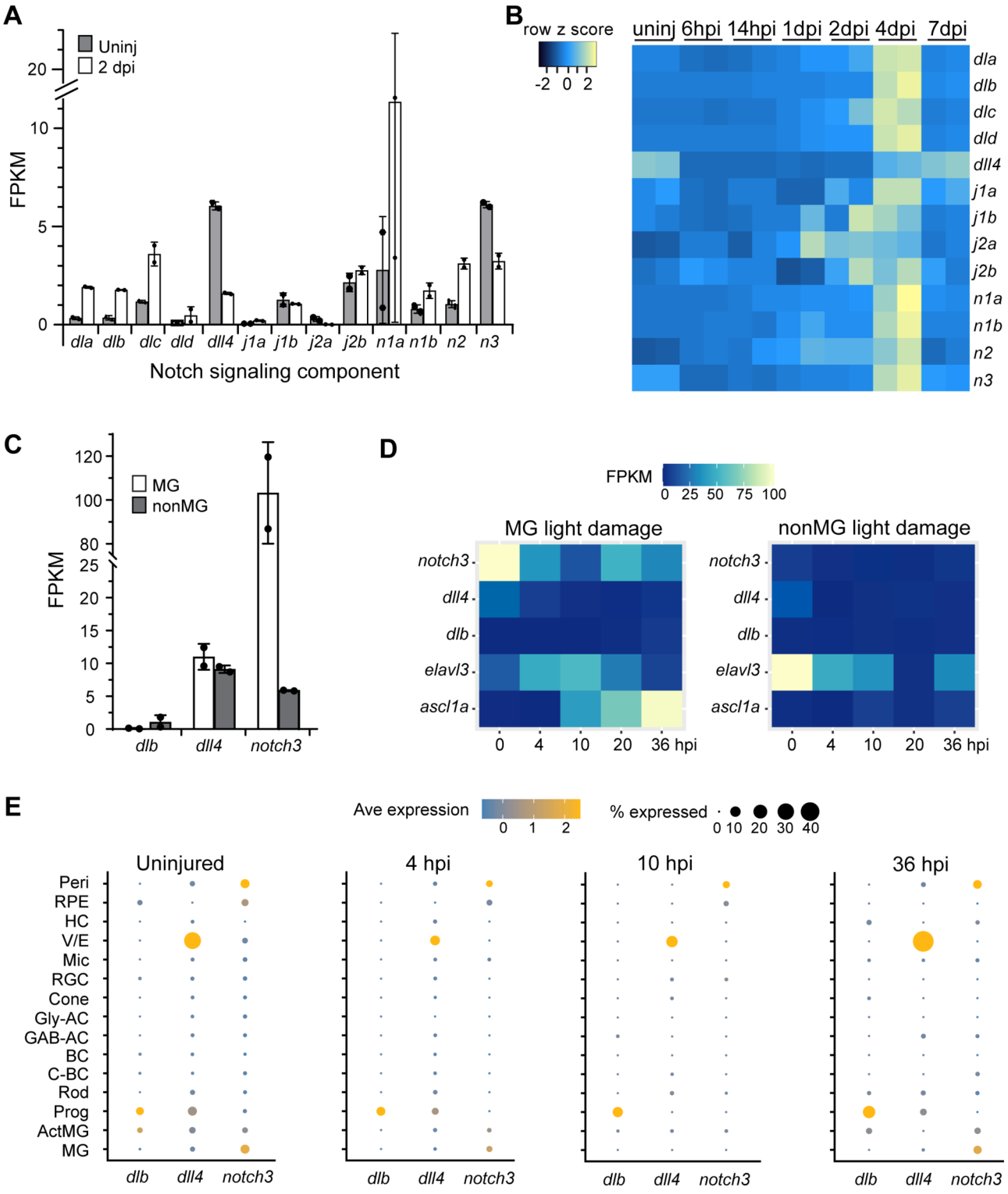

GLIA_24075_Figure_5.tif

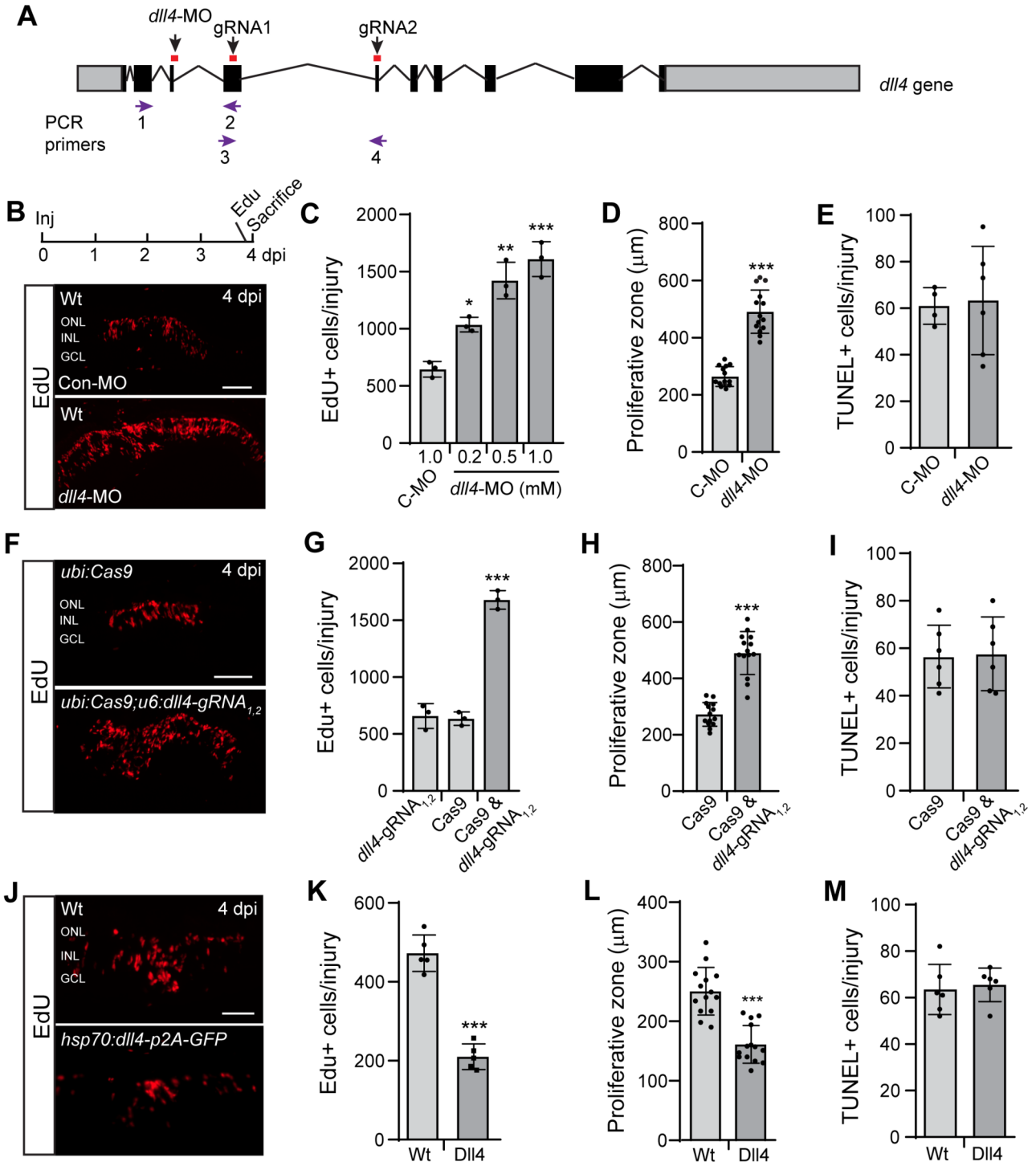

GLIA_24075_Figure_6.tif

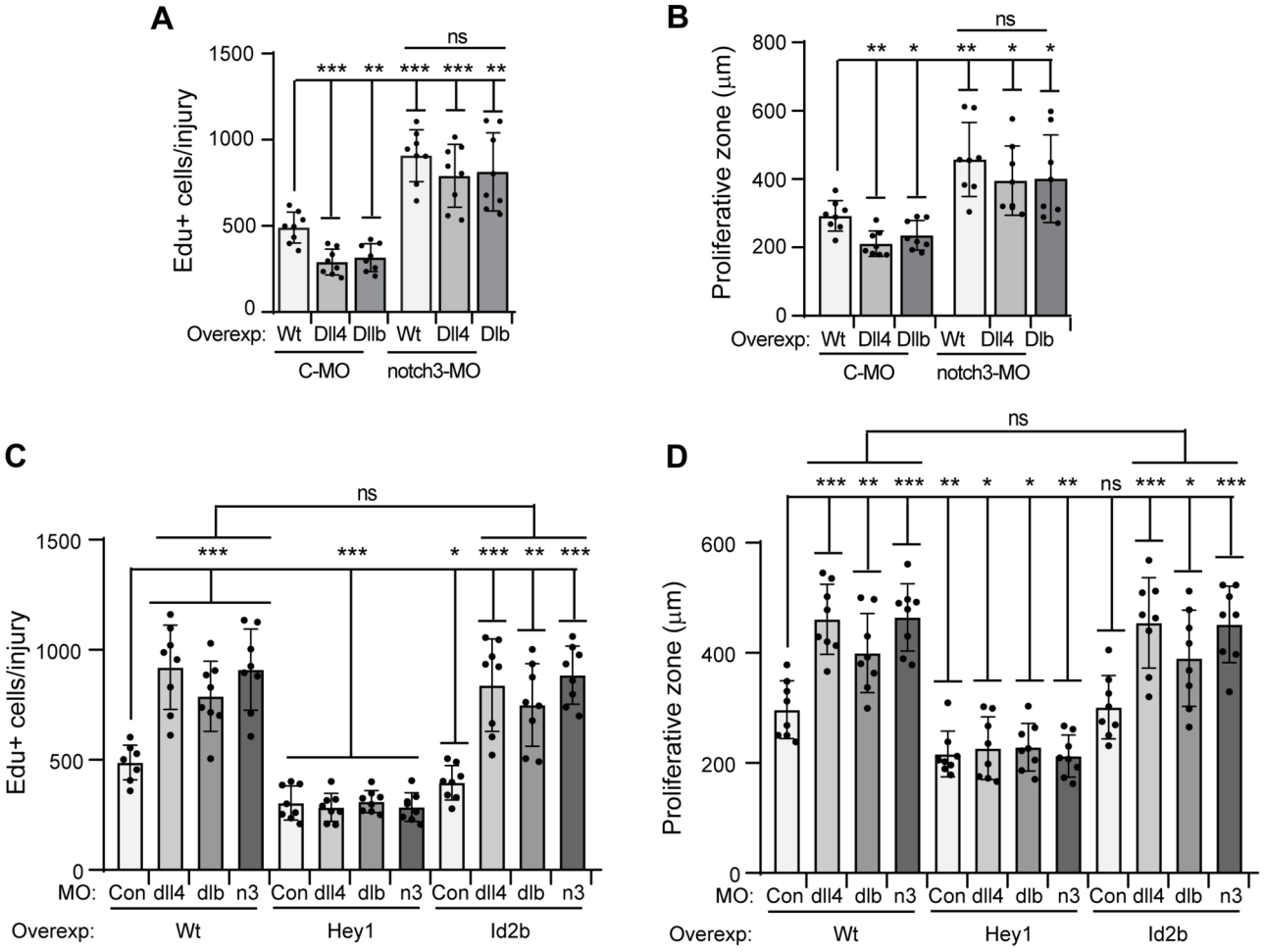

GLIA_24075_Figure_7.tif

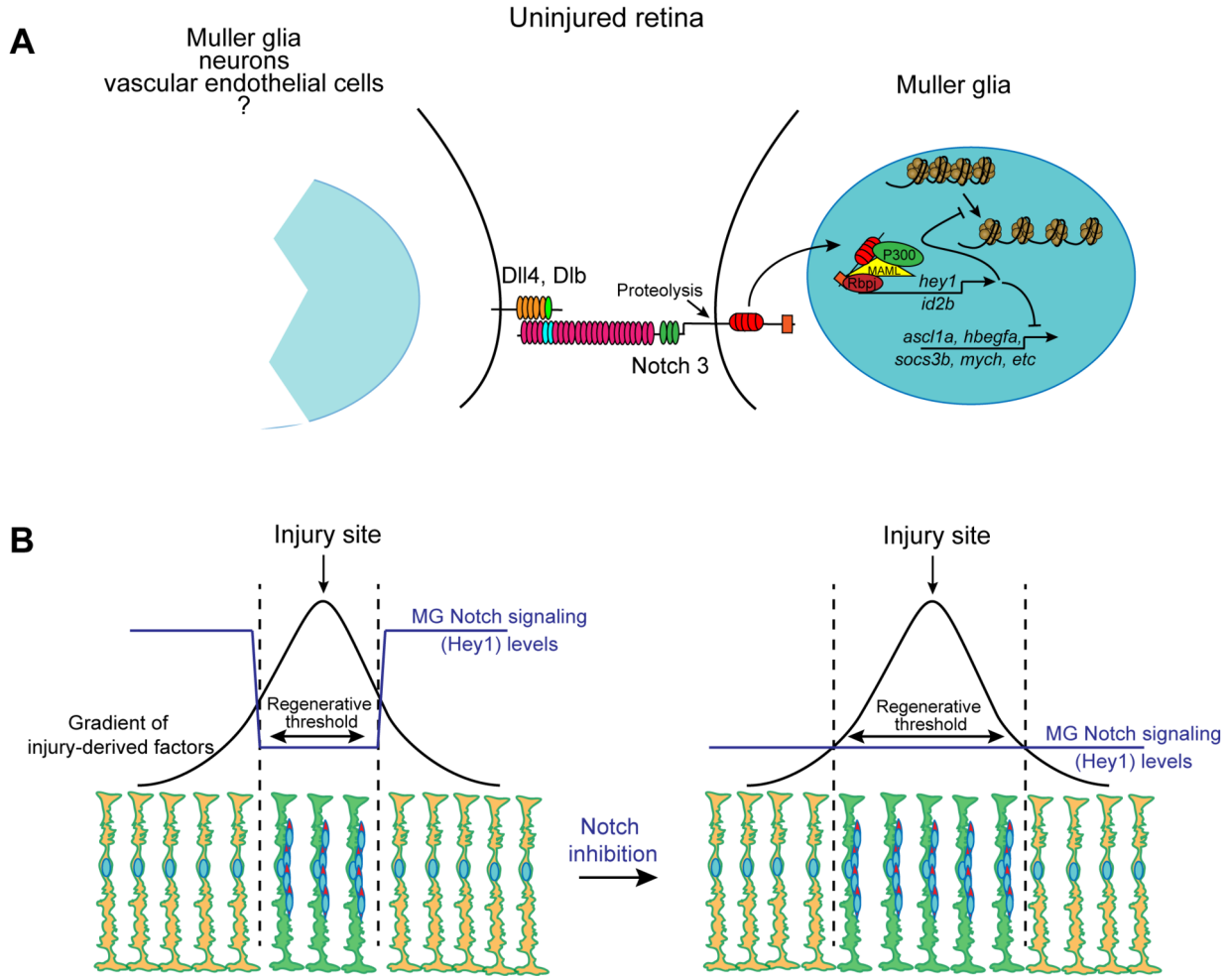

GLIA_24075_Figure_8.tif

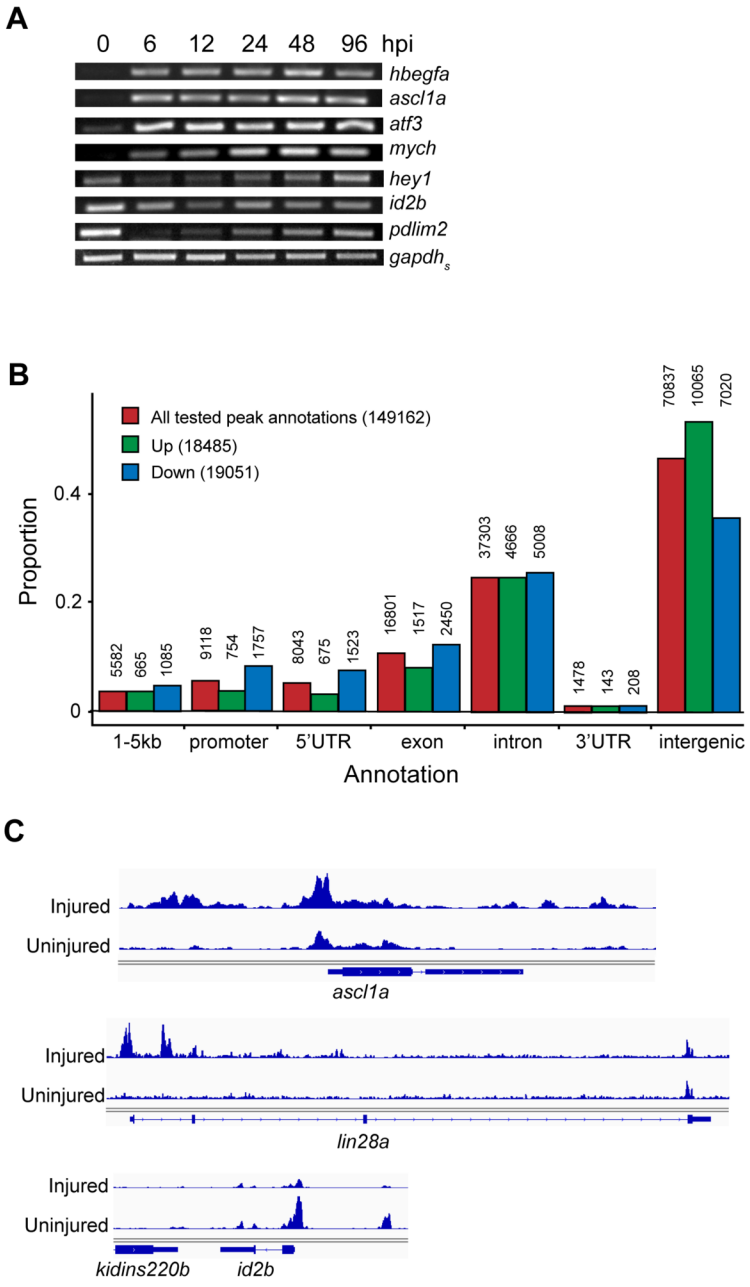

GLIA_24075_Figure_supplement_1.tif

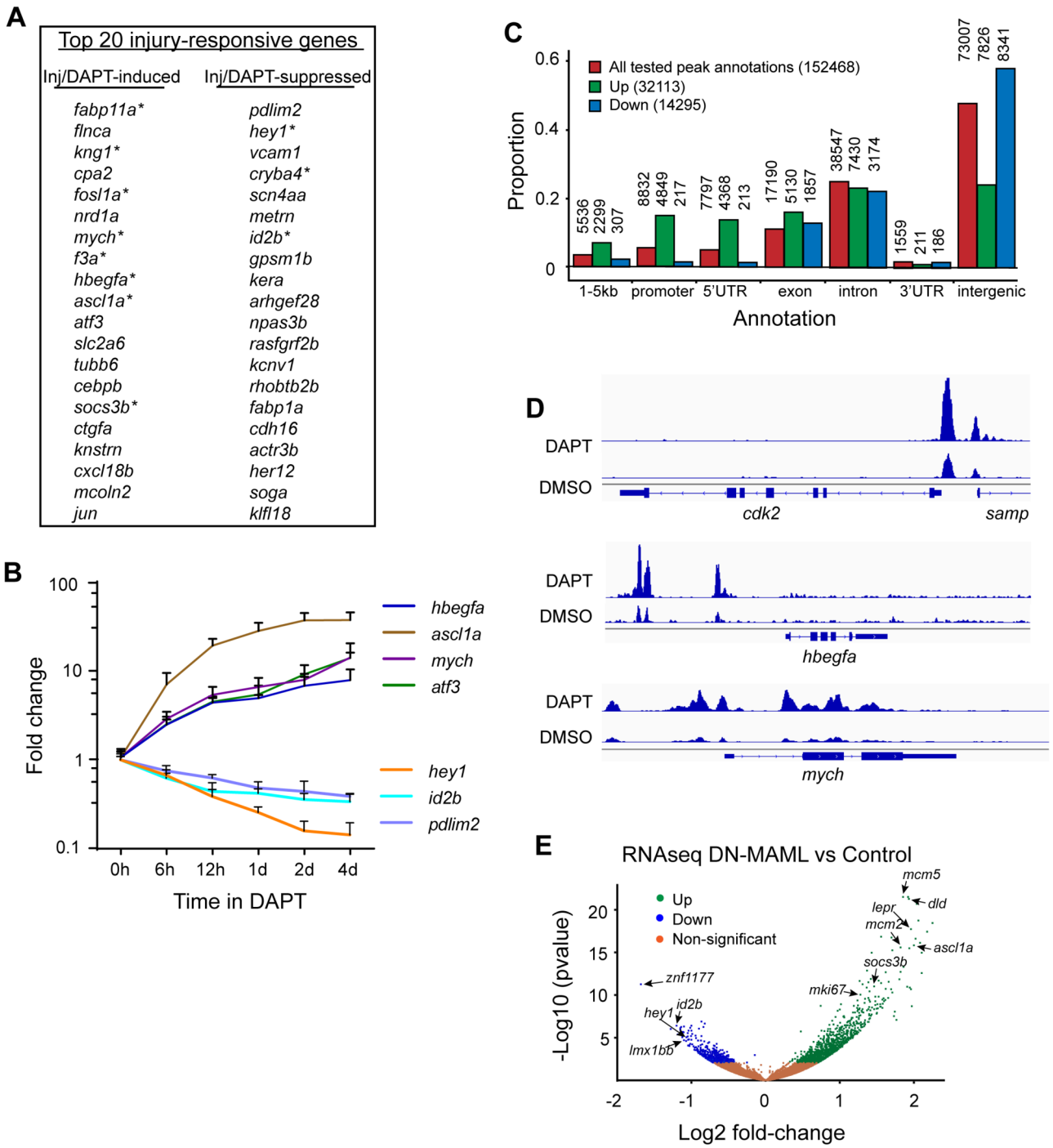

GLIA_24075_Figure_supplement_2.tif

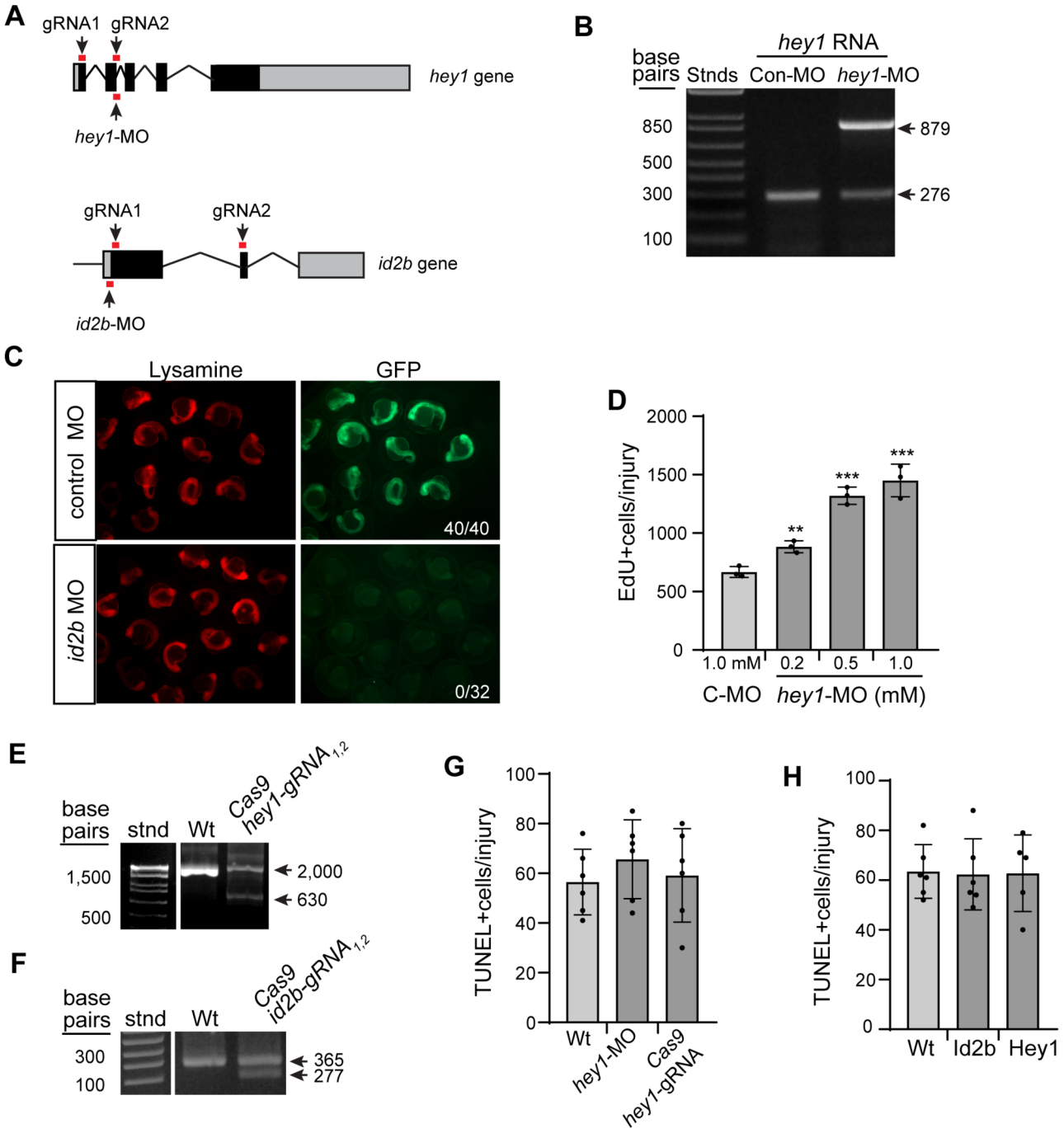

GLIA_24075_Figure_supplement_3.tif

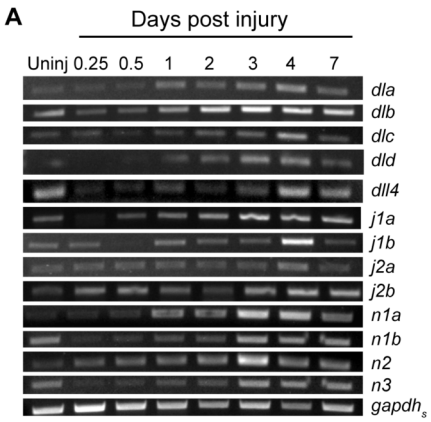

B

Cell type	*dlb (%)*	*dll4 (%)*	*notch3 (%)*	Total cells
Resting MG	4 (0.05)	53 (0.68)	334 (4.3)	7738
Activated MG	116 (1.7)	34 (0.49)	104 (1.51)	6905
Neurons	40 (0.16)	91 (0.36)	61 (1.51)	25395
Microglia	5 (0.20)	2 (0.08)	5 (0.20)	2520
V/E	0 (0)	95 (22)	2 (0.47)	427
Progenitors	19 (4.3)	16 (3.59)	1 (0.22)	446

scRNAseq data from Hoang et al., 2020 was interrogated for gene expression data. Values are the number of cells exhibiting expression above background in the uninjured retina.

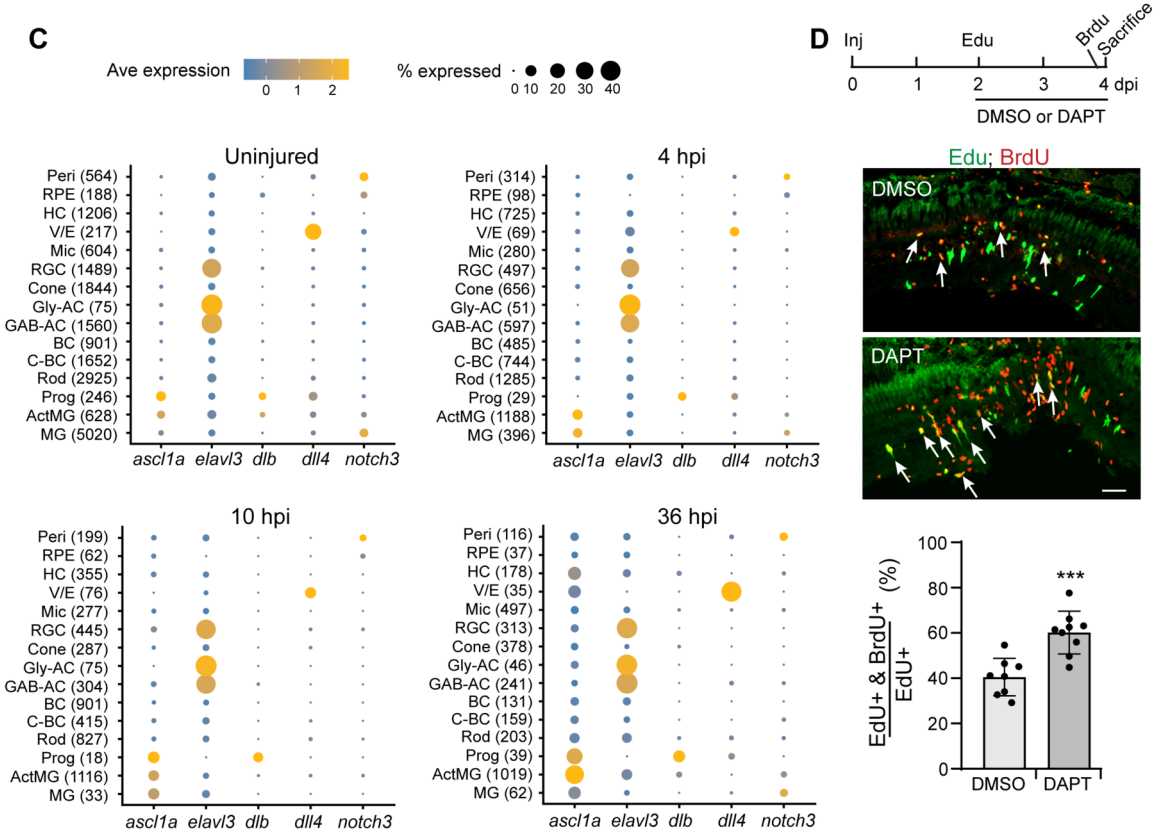

GLIA_24075_Figure_supplement_4.tif

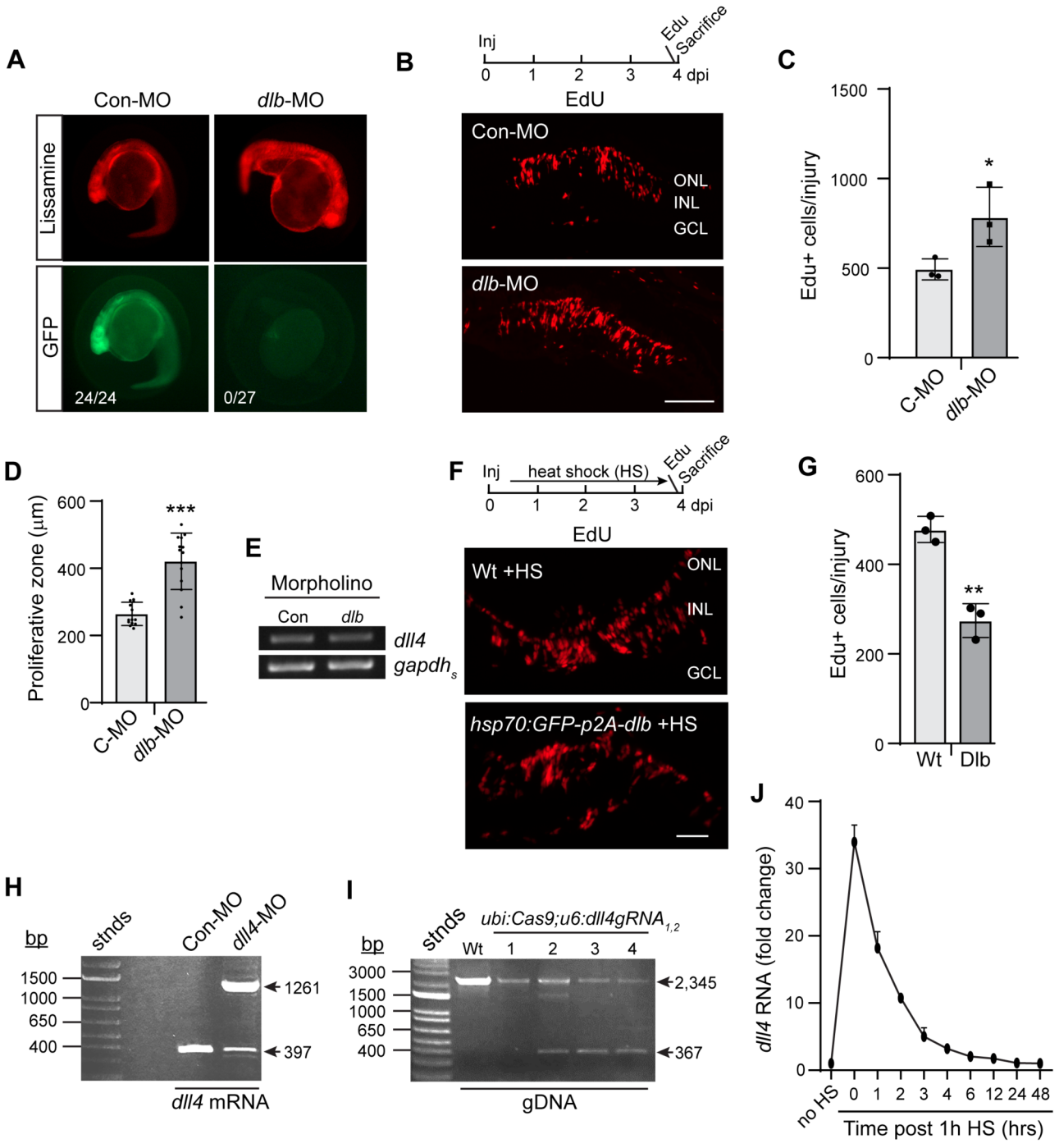

GLIA_24075_Figure_supplement_5.tif

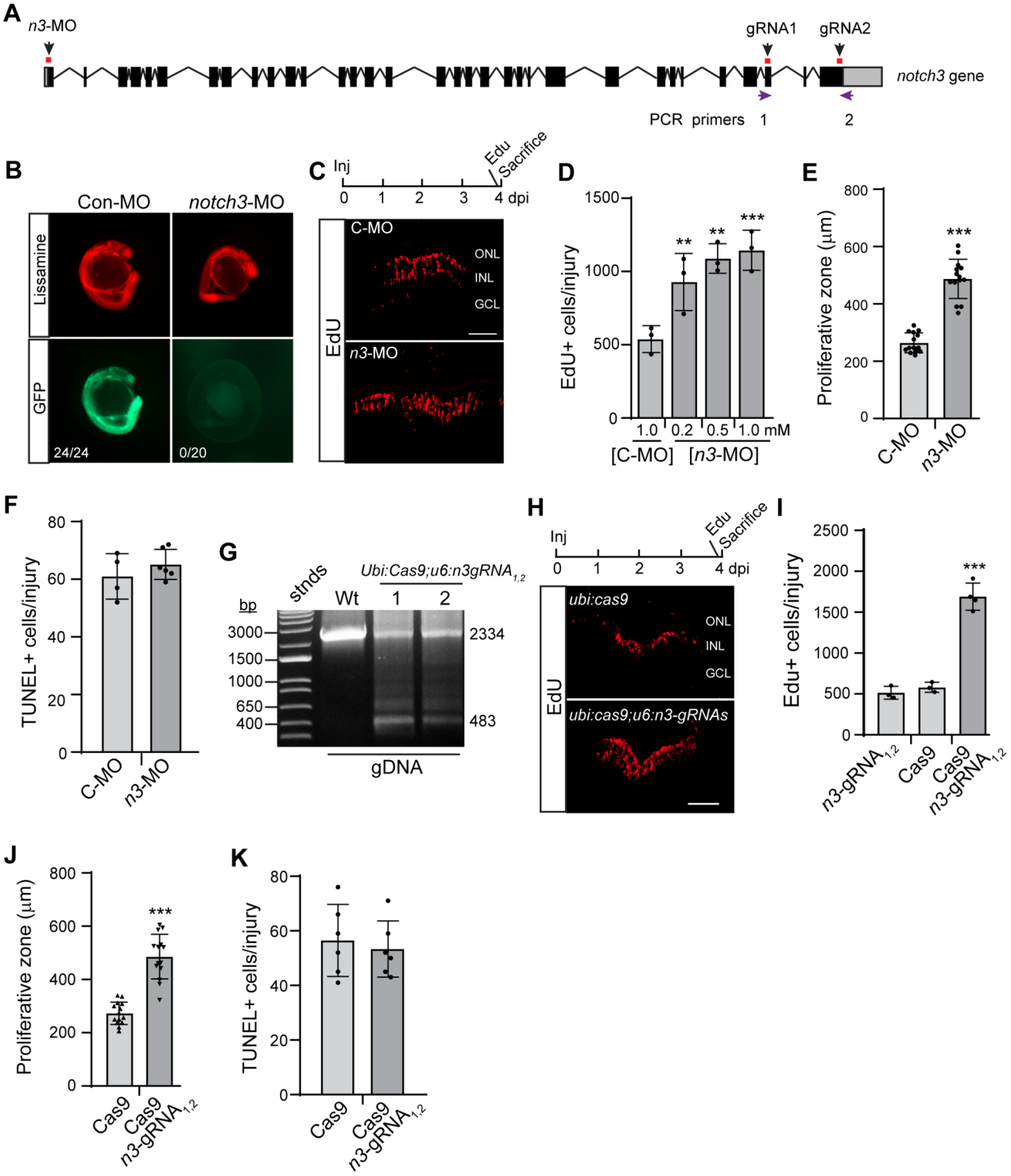

GLIA_24075_Figure_supplement_6.tif

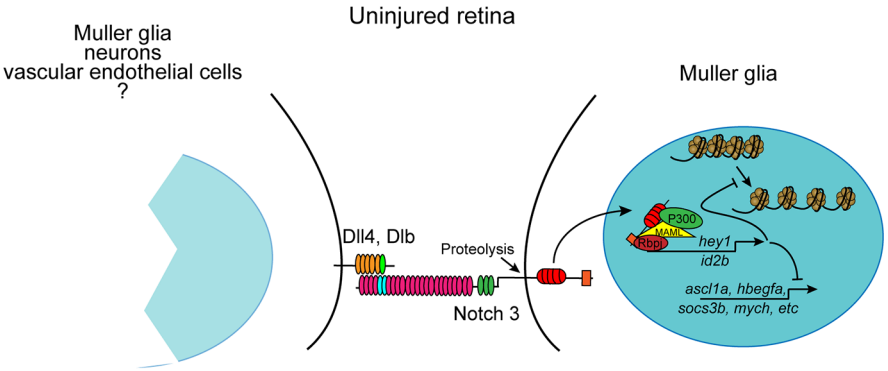

GLIA_24075_TOC image.tif